Electrochemical and Electrostatic Energy Storage and Management Systems for Electric Drive Vehicles: State-of-the-Art Review and Future Trends

Ephrem Chemali, *Student Member, IEEE*, Matthias Preindl, *Member, IEEE*, Pawel Malysz, *Member, IEEE*, and Ali Emadi, *Fellow, IEEE*

***Abstract*— Recently, increased emissions regulations and a push for less dependence on fossil fuels are factors that have enticed a growth in the market share of alternative energy vehicles. Readily available energy storage systems (ESSs) pose a challenge for the mass market penetration of hybrid electric vehicles (HEVs), plug-in HEVs, and EVs. This is mainly due to the high cost of ESS available today. However, tremendous research efforts are going into reducing the cost of these storage devices, increasing their lifespan, and improving their energy density. This paper aims to give an overview of the current state of readily available battery and ultracapacitor (UC) technologies as well as a look ahead toward promising advanced battery chemistries and next generation ESS. Energy management systems and various battery balancing configurations are discussed in addition to battery state/parameter estimation and protection mechanisms. Finally, hybrid ESSs (HESS) are reviewed as a mitigation strategy to the shortcomings of traditional battery and UC technologies. Consideration is given to the combination of advanced battery chemistries with UCs to portray HESS performance, which can meet and exceed the performance of current ESS technologies.**

***Index Terms*— Battery balancing, battery management systems (BMSs), battery modeling, battery technology, energy management systems (EMSs), energy storage system (ESS), hybrid ESSs (HESSs), Li-ion batteries, ultracapacitors (UCs).**

I. Introduction

In THE absence of any policy change, the International Energy Agency (IEA) predicts a 70% increase in oil consumption and a 130% increase in CO_2 emissions by 2050, raising the global average temperature by 6 °C [1]. In order to reduce global CO_2 emissions to 2008 levels by 2050, an injection of U.S. $17 trillion in investments is needed by 2050. This amounts to an average of U.S. $400 billion of investments in clean energy technologies per year by 2050 [1]. The research, development, and commercialization of these energy efficient technologies require not only significant investments from the private sector but from the public sectors as well. Other factors, which will accelerate implementation of these technologies, are new and stricter regulations, government incentives, and a change in public opinion. The transportation sector contributes significantly to the increase in oil demand and CO_2 emissions. The IEA claims that in order to simply curtail the CO_2 emissions to 2008 levels by 2050, a drastic change must occur in the transportation industry. These changes will involve alternative energy vehicles to dominate the light-duty vehicle market and an increase of 50% in fuel economy by 2050 [1].

These alternative fuel vehicles, which include hybrid electric vehicles (HEV), plug-in HEVs (PHEVs), and EVs, which, in general, are referred to as XEV, have the added benefit of an electrified powertrain, offering much greater efficiencies than its counterpart, the internal combustion engine. In addition to being more efficient, electrified powertrains are able to recapture breaking energy that is, otherwise, wasted through mechanical breaks. The primary components in an electric propulsion system are the motor/generator, the battery/ultracapacitor (UC) pack or energy storage system (ESS), and the power electronics drive system. The latter ensures the energy conversion and transfer between the electric machine and the ESS [2], [3]. Battery technology is one of the major barriers to the mass market adoption of XEV. As such, battery technologies are being extensively researched nowadays and the industry's landscape is rapidly changing.

This paper aims to offer an overview of the current state of battery/UC technologies, energy management systems (EMSs), as well as hybrid ESSs (HESSs) for electric drive vehicles. First, current prevalent battery/UC cell chemistries will be discussed and an overview will be given on advances in UC and Li-ion battery technology. Second, EMSs, which includes protection, state/parameter estimation, and balancing, are discussed. And finally, the benefits offered by HESS are discussed as well as an overview of prevalent HESS topologies.

II. Cell Technologies

Nowadays, most research efforts in battery technology are geared toward increasing specific energy and reducing cost

Manuscript received December 12, 2015; revised February 28, 2016; accepted April 19, 2016. Date of publication May 10, 2016; date of current version July 29, 2016. This work was supported by the Canada Excellence Research Chair in Hybrid Powertrain Program. Recommended for publication by Associate Editor X. Ruan.

E. Chemali, P. Malysz, and A. Emadi are with the Department of Electrical and Computer Engineering, McMaster Institute for Automotive Research and Technology, McMaster University, Hamilton, ON L8S 4K1, Canada (e-mail: chemale@mcmaster.ca; malyszp@mcmaster.ca; emadi@mcmaster.ca).

M. Preindl is with the Department of Electrical Engineering, Columbia University, New York, NY 10027 USA (e-mail: matthias.preindl@columbia.edu).

Color versions of one or more of the figures in this paper are available online at http://ieeexplore.ieee.org.

Digital Object Identifier 10.1109/JESTPE.2016.2566583

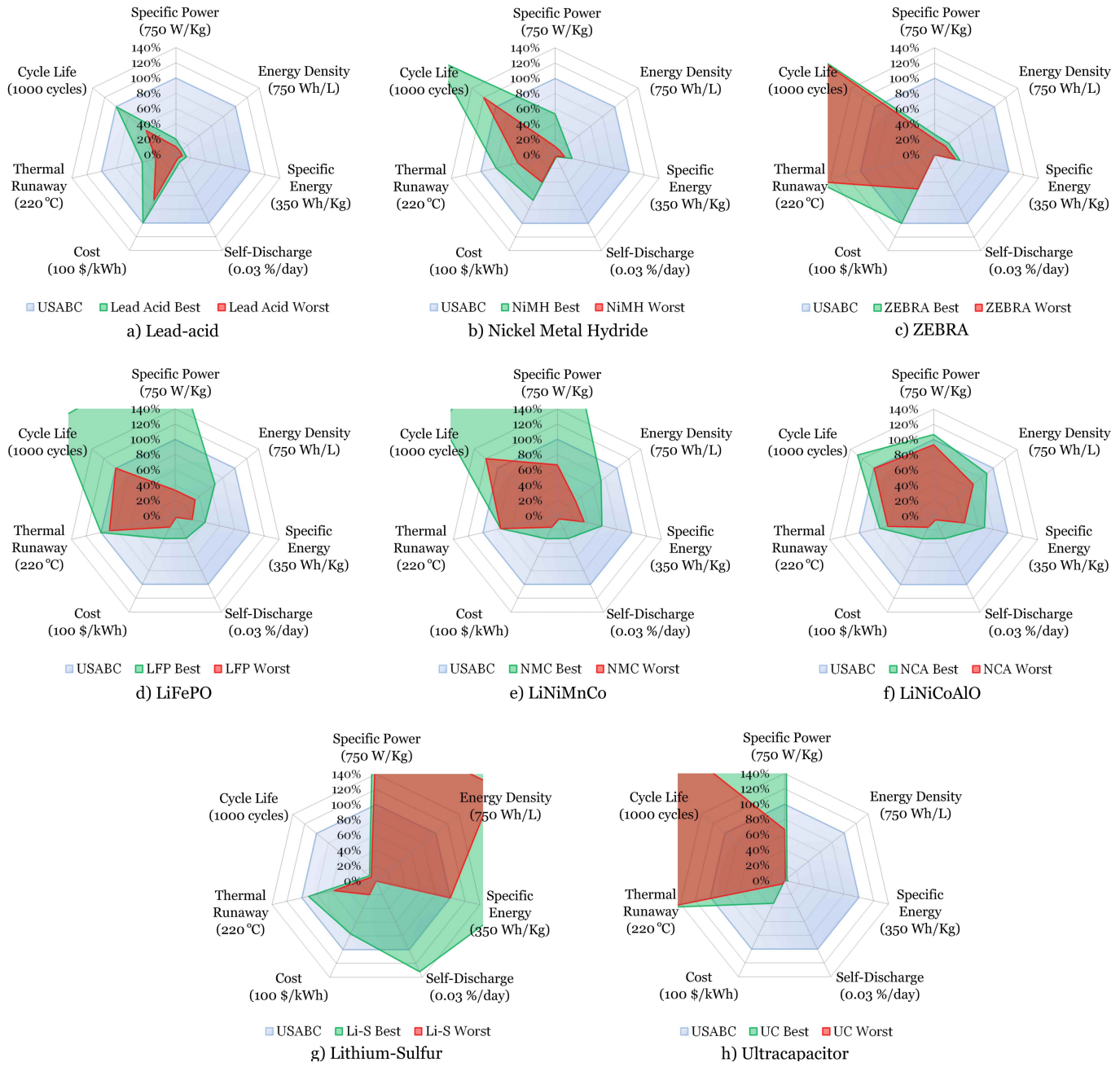

Fig. 1. Spider plots of prevalent battery technologies. (a) Lead acid. (b) Nickel metal hydride. (c) ZEBRA. (d) LiFePO. (e) LiNiMnCo. (f) LiNiCoAlO. (g) Lithium–sulfur. (h) UC.

while maintaining a high cycle life. The U.S. Advanced Battery Consortium (USABC) has set specific goals to be reached by 2020 for pure EV battery packs. These include a specific energy, at cell level, of 350 Wh/kg, a cost of $100/kWh at the production volumes of 100 000 45 kWh units, and a cycle life of 1000 cycles. In the automotive industry, the end of life of a battery marks the number of charge/discharge cycles, which the battery undergoes before it reaches 80% of the initial battery capacity.

In this section, readily available cell technologies are discussed and compared. Each cell chemistry is evaluated on seven different metrics and compared with the USABC 2020 goals, shown in Fig. 1. Safety as a performance metric is not particularly outlined in the USABC goals; however, this is a critical metric in the light of the recent incidents associated with batteries. Therefore, the USABC goals have been augmented to include the onset temperature of thermal runaway for each cell technology as an indicator of safety [13], [24], [25], [27]–[31]. A score of 0% to 100% for each metric is given to the cell technology depending on how well it meets the augmented USABC goals. The metrics used are energy density (Wh/L), specific energy (Wh/Kg), specific power (W/Kg), self-discharge (% of initial cell capacity per day), cost ($/kWh), cycle life (cycles), and safety.

TABLE I
EXISTING BATTERY AND UC SPECIFICATIONS

Specifications	Augmented USABC	Lead Acid	Nickel Metal Hydride	ZEBRA	Ultracapacitor
Specific Power (W/Kg)	700	75 - 150 [4]	80 - 400 [4]	150 - 200 [5], [6]	500 - 100,000 [7], [8]
Energy Density (Wh/L)	750	50 - 80 [7]	60 - 150 [7]	135 - 180 [5], [7]	10 - 30 [7]
Specific Energy (Wh/Kg)	350	30 - 50 [7], [8]	45 - 80 [9]	100 - 120 [5], [7]	2.5 - 15 [7]
Self-Discharge (%/day)	0.03	0.29 - 0.57 [4]	1 - 1.43 [4], [10]	15 [7]	20 - 40 [7]
Cost ($/kWh)	100	100-150 [11]	150 - 250 [2], [9]	100 - 200 [7]	300 - 2000 [7]
Cycle Life (cycles)	1000	500 - 1000 [7]	1200 - 2000 [12]	>2500 [7], [8]	>100,000 [7], [8]
Thermal Runaway (^{o}C)	220 [a]	60 - 100 [13], [14]	110 - 175 [8]	- [b]	- [c] [15]

[a]Added to USABC goals
[b]ZEBRA batteries operate at temperatures larger than 270 °C
[c]Cell vented before thermal runaway onset temperature was reached

TABLE II
LI-ION BATTERY SPECIFICATIONS

Specifications	Augmented USABC	$LiFePO_4$	LiNiMnCo	$LiNiCoAlO_2$	Li-S
Specific Power (W/Kg)	700	250 - 1600 [4]	500 - 2400 [4]	700 - 800 [4], [16]	1500 - 3000 [17]
Energy Density (Wh/L)	750	250 - 500 [7], [18]	230 - 550 [7], [18]	500 - 670 [7], [19]	1500 - 2600 [7], [19]
Specific Energy (Wh/Kg)	350	80 - 140 [4], [16]	126 - 210 [16], [18]	145 - 240 [19], [20]	350 - 600 [17], [18]
Self-Discharge (%/day)	0.03	0.1 - 1.29 [4], [7]	0.1 - 0.71 [4], [7]	0.1 - 0.57 [4], [7]	0.025 - 32 [21]
Cost ($/kWh)	100	300 - 600 [22]	300 - 600 [22]	300 - 600 [22]	>130 [a] [19]
Cycle Life (cycles)	1000	1000 - 2000 [16]	1200 - 1950 [16], [23]	1000 - 1280 [16], [20]	80 - 110 [16], [23]
Thermal Runaway (^{o}C)	220 [b]	195 [24]	168 [24]	136 - 160 [25]	125 - 200 [26]

[a]Estimation based on cited work
[b]Added to USABC goals

A summary of each cell chemistry's performance and specifications is given in Tables I and II. The data outlined in Tables I and II, which are also shown in Fig. 1, were obtained after an extensive investigation of the existing battery/UC technology literature. Particular attention was mostly paid to the literature, which obtained experimental results for each one of the seven metrics considered in this paper. For each metric of each battery/UC technology, there typically exists more than one experimental value reported in the literature. The maximum and minimum values for each one of these metrics for each cell technology are outlined in Tables I and II. These minimum and maximum values are used to generate the green and red plots, shown in Fig. 1, to portray a technology's best and worst performance, respectively.

A. Nickel Metal Hydride Batteries

Nickel metal hydride (NiMH) batteries, whose performance data are shown in Fig. 1(b) and in Table I, have been used in HEVs for 14 years. Prominent cell manufacturers of NiMH include PEVE and Sanyo Electric (Panasonic). The technology has been well developed and has shown durability in vehicles, such as the NiMH RAV4 EV, which has been in operation for over ten years [32]. Electrochemically, the negative electrode is hydrogen that is absorbed/released in an intermetallic compound. The positive electrode is composed of nickel compounds and the electrolyte is typically an aqueous solution of 30 wt% potassium hydroxide [33]. Commercially available cells are produced in both cylindrical and prismatic hard case variants and span a voltage of 1.2–1.35 V [33]. Coulombic efficiency is about 10% less than that of the lead-acid batteries [33]; however, NiMH power/energy capabilities are far greater, typically factors of two to three times the power/energy density of lead acid. NiMH technology's shortcomings lie in their significantly higher self-discharge rate [33], which does not allow them to be ideal candidates for energy-oriented applications, such as PHEVs and EVs. Recent advances in NiMH include the usage of bipolar cell designs to increase power [34].

B. ZEBRA Batteries

The origins of the sodium nickel battery, also called the ZEBRA battery, are traced back to South Africa, where the first patent was awarded for this technology in 1978 [35]. In 1984, the first EV to be powered by a ZEBRA battery was driven in Derby, U.K. The technology has been in development since then and has matured. Commercially available ZEBRA batteries, whose performance data are shown in Fig. 1(c), are based on sodium nickel chloride (Na–Ni–Cl) electrochemistry where sodium is the negative electrode and nickel chloride is the positive electrode. ZEBRA batteries operate at a temperature of 270 °C to 350 °C [36], since sodium is found in its molten state at these temperatures. As a result, these batteries are more commonly referred to as molten salt batteries. The cells are manufactured in an upright rectangular box format. Special pack design and thermal considerations are needed to maintain the high operating temperature. As a result, the energy required to maintain operating temperatures result in a self-discharge. Some advantages

of this technology include a relatively high specific energy of 90–120 Wh/kg [5], [7] shown in Table I, their insensitivity to ambient temperature, and fault tolerance. The latter is due to the cells having a low resistance short-circuit state when cell damage occurs, allowing continuous operation during cell failures [5], [35]. This makes them operationally safe and good candidates in harsher climates. In addition, they have a near 100% Coulombic efficiency [35], [37] and a cycle life measured to be over 2500 cycles [8], [35]. These batteries have better energy density and specific energy than NiMH, and their power capabilities and pack cost are less. However, their higher self-discharge rate measuring at 15% [7] per day is an order of magnitude larger than the other electrochemical devices considered in this paper. Applications, which have employed ZEBRA batteries, include European EVs, such as Think EV, Iveco Electric Daily, and Modec EV vans.

C. Li-Ion Batteries

Battery technology has come a long way in the last few decades. Li-ion battery technology powers most mobile applications from smartphones and laptops to, nowadays, ESSs for electric drive vehicles and smart-grid applications. In the case of XEVs, Li-ion batteries are energy dense and, therefore, allow the vehicle to have a longer electric-only driving range; however, they typically do not have the specific power to provide or accept large power spikes, resulting from the dynamic power profile of a vehicle. During a regenerative braking scenario, Li-ion batteries are limited in terms of the power levels, which they can handle; therefore, a large portion of the regenerated energy is dissipated through the mechanical brakes. Under highly dynamic power profiles, the battery of an XEV can be greatly overstressed, which negatively affects the longevity of its lifespan. Highly dynamic load profiles imposed on the battery pack induces degradation at the cell level, which leads to increased internal resistance. Capacity fade is also a consequence of this phenomenon, which most often results in premature cell end of life or even premature failure [38].

There are various materials used in the construction of Li-ion cell electrodes. The cathode materials are usually oxide variants of lithium metal amalgams, which usually contain either manganese (LMO), cobalt (LCO), nickel, iron–phosphate (LFP), or mixtures thereof, such as LiNiMnCo (NMC) and $LiNiCoAlO_2$ (NCA), containing an aluminum blend [39]. Anode materials are typically graphite, although hard carbon, silicon–carbon compounds, lithium titanate, tin or cobalt alloys, and silicon–carbon blends have also been used in consumer electronics. In all varieties, lithium ions transport back and forth between the electrodes and transfer electrons in an intercalation-based reaction instead of a traditional molecule-to-molecule chemical reaction. The benefits of Li-ion technology are higher cycle life [16], [20], high Coulombic efficiency (up to 98%) [39], and low self-discharge [4], [7]. A wide variety of electrolyte materials are also possible from solid-based to liquid-based, usually of the organic nonaqueous form. The usage of lightweight materials and the high voltage potential of lithium-ion electron transfer give rise to high power/energy densities and some of the highest electrochemical cell nominal voltages, e.g., 3.2–3.8 V [34], [40]. The LiFePO (LFP) variant, whose spider plot is shown in Fig. 1(d), is considered to be among the safest Li-ion cell chemistries due to its higher thermal runaway temperature [39]. Meanwhile, NMC and NCA cells are dominating the EV market nowadays given their stronger power/energy performance when compared with other technologies, as can be observed in Fig. 1(e) and (f) and Table II. As a result, companies, such as Panasonic, Tesla, LG Chem, and Samsung SDI, are heavily investing in these two cell chemistries.

Nowadays, Li-ion chemistries are being extensively researched and developed to significantly increase energy and power capabilities as well as operating voltage. For example, improvements in NMC cathodes have shown an increase in operating voltage from 4.13 to 4.3 V [41]. In addition, operating voltages of up to 4.7–4.8 V have been observed in lithium vanadium phosphate cathodes, which have been integrated into the Subaru 64e prototype [42]. Although, some members of the research community are focusing on incremental improvements in the conventional Li-ion chemistries, many others are betting on a leap in technology embodied by the next generation Li-based battery cells that have the capability to significantly outperform the conventional Li-ion cells.

D. Advances in Li-Based Battery Technologies

Conventional Li-ion battery technology has a theoretical specific energy of 387 Wh/kg [43], [44]. Commercial cells manufactured, nowadays, are approaching a specific energy of 240 Wh/kg [40], and thus, it is clear that the current Li-ion battery technology is reaching its limits. If mass marketed EVs are to ever reach a driving range of over 500 km per charge, the dawn of a new age in commercial battery technology must come about.

Li–Air (Li_2O_2) and Li–S chemistries have been gaining a great deal of interest from the research community primarily due to their very high theoretical specific energy of 3582 and 2567 Wh/kg, respectively [44], [45]. In addition, Li–Air and Li–S cathodes are composed from abundantly available materials, such as O_2 and elemental sulfur, respectively, which would render these cells cheaper to manufacturer. Both of these battery technologies posses the same metallic Lithium anode where Li is oxidized when a load is observed in the external circuit. Lithium ions then travel across the electrolyte to reduce oxygen or elemental sulfur in the cathode of Li–Air and Li–S cells, respectively. Much of the increased theoretical energy density of these batteries is a consequence of its pure metallic lithium anode, which can hold more charge than lithiated graphite anodes per unit mass found in traditional Li-ion batteries [44], [46]. Furthermore, the cathode in readily available Li-ion batteries, such as the cathode in the $LiCoO_2$ cells store less lithium than Li_2O_2 or Li_2S cathodes [44], [46].

In Li–Air cells, Li ions react with O_2^{-2}, which is reduced from O_2 in surrounding air. Initially, unwanted discharge products form due to Li ions reacting with other molecules within air, such as CO_2. As a result, Li–Air cells are wrapped with various types of membranes to increase their

permeability to O_2. A key and important factor inhibiting commercialization of these cells is electrolyte degradation giving rise to poor lithium cycling efficiencies and capacity fading [44], [46]–[48]. Currently, research on Li–Air cells shows as much as 50% capacity fade after only 20 discharge cycles [44].

Similarly, Li–S cells suffer from poor sulfur cycling efficiencies, which lead to fast capacity fading [17], [44]. In addition, sulfur is a good insulator, thus leading to poor electrode kinetics and limited discharge rates [44], [46], [49]. Currently, Li–S prototype cells experience as much as 50% capacity fade after 50 discharge cycles [44]. This and other performance specifications of Li–S are shown in Fig. 1(g) and in Table II. Sion Power is one of a few privately held companies, which is developing this technology. They currently claim having developed Li–S cells with a specific energy of 350 Wh/kg and predict that this value will increase to 600 Wh/kg in the future [50].

Some advances have been made recently to accelerate the advent of Li–Air and Li–S batteries. These studies have focused primarily on replacing traditional carbon–S cathodes with graphene–S cathodes. Graphene has a high electrical conductivity and has a large surface area, which can lead to improved cycle life [43], [51]–[55]. Using graphene, a capacity fade of under 30% after 100 cycles is being reported by some studies [43]. Recently, silicon is also being considered as an alternative to graphite-based anode materials to address the issue of capacity fading in Li-based battery technology [56]–[59]. One study reported a capacity fade of only 3% after 1000 cycles by constructing the electrode from pomegranate-shaped silicon-carbon structures [59].

E. Ultracapacitors

Traditional capacitors are composed of two electrodes with a middle separator made of solid dielectric material. Energy is stored in the form of electrostatic potential when the two plates become oppositely charged. Typically, the solid dielectric materials chosen are ceramics and metal oxides [2]. The lack of faradaic processes results in a terminal voltage that is directly proportional to the state of charge (SOC) [60]. While the plates accumulate charge, the dielectric material's molecular dipoles, which find themselves antiparallel to the electric field, will feel a torque that realigns them with the electric field. As a result, capacitance is dependent on surface area of the electrode, the dielectric constant, and the separation distance between plates, as follows:

$$C = \frac{A\epsilon}{d}. \tag{1}$$

UCs or supercapacitors are different than traditional capacitors, since they employ two forms of energy storage: electrostatic storage and electrochemical storage. Furthermore, instead of having a solid dielectric material separating both electrodes, they possess an electrolytic solution. Energy storage in the form of electrostatic potential is called the electric double-layer capacitance [61]. This is also, sometimes, referred to as a Helmholtz double layer due to Helmholtzs' discovery of the double layer of charge, which accumulates at the interface between electrode surface and electrolyte. One layer develops in the form of charge on the electrode, while a second layer develops in the form of ions, which diffuse from the electrolytic solution to the surface of the electrode. This diffusion process is very similar to the one, which occurs within Li-ion batteries. The charge on the electrode surface must be equal and opposite to the charge accumulated on the electrolyte layer as a result of electroneutrality. The layer of charge formed on the electrode surface is typically less than 1 Å(0.1 nm) thick, while the layer of charge on the electrolyte phase is much harder to model due to its complex structure [62]. The electric double layer, which forms at the interfacial region of both electrodes, can be modeled as a capacitance [61].

Energy storage in the form of electrochemical potential is the second form of energy storage utilized in some UCs. This form of energy storage, called pseudocapacitance, is achieved when ions in the electrolyte diffuse to the electrode–electrolyte interface where they adsorb into the electrode lattice structure [61], [63], [64]. Other processes have been used to achieve pseudocapacitance; these include redox reactions of ions within the electrolyte, and doping of active polymers in the electrode [61]. In the case of pseudocapacitance through adsorption, intercalation and electrodeposition can occur at the surface whereby product ions, such as Li^+, are incorporated into the electrode lattice. While undergoing adsorption, the ions give up or receive electrons through oxidizing and reducing reactions [61], [65].

In the case of electric double-layer capacitors (EDLCs), energy is stored in the electric double layer rather than in faradaic processes. Ions in the electrolyte diffuse toward the electrode surface and can integrate into the porous lattice [2], [61]. On the other hand, pseudocapacitors use only faradaic redox reactions as their main form of energy storage [2], [61]. Charge transfer is observed between the electrolyte phase and the electrode phase. Pseudocapacitors present higher energy densities than traditional EDLC but they also have their drawbacks. These are primarily due to their reliance on processes, such as adsorption and electrodeposition into the electrode structure during charge transfer processes, which increases wear and deterioration of the lattice structure and, therefore, lends to shorter life cycles. So far, manufacturers have only been able to produce cells with only one out of the two electrodes being pseudocapacitive [61]. These are more commonly referred to as hybrid asymmetric UCs. Two of the most advanced hybrid UC cells available on today's market are the Yunasko 5000F cell and the JM energy Ultimo 1100F cell. According to a study done at the U.C. Davis Institute of Transportation Studies, these cells, in their laminated pouch form, possess a specific energy of 30 and 10 Wh/Kg while maintaining a specific power of 3395 and 2450 W/Kg, respectively [66]. Performance data of ultracapcitors are shown in Fig. 1(h) and in Table II.

As will be discussed in greater detail in Section V, ultracapcitors are being strategically used to enhance ESS power and lifetime capabilities by buffering the battery and enabling greater acceleration and regenerative braking capabilities. Maxwell UCs are being employed in hybrid buses and in PSA

microhybrids [42], [67]. A new Mazda-6 model uses a UC to enable regenerative braking on a 12 V start–stop microhybrid. Honda, Toyota, and AFS Trinity have each developed concept/prototype vehicles to enable higher performance through the use of UCs.

III. Energy Management Systems

An EMS is a system for protection, estimation, and control of a battery, UC, or HESS to ensure safe high-performance operation and a long lifetime [68], [69]. ESS consists of multiple cells that are connected in series and/or in parallel. Cells are connected in series to obtain a rated voltage of the pack. Parallel connections increase the rated capacity of a pack, such that the required amount of charge, i.e., energy, can be stored. Also, adding parallel cells increase the rated current, i.e., power, of a pack.

Large packs for XEV consist of hundreds or thousands of cells. To simplify the arrangement, packs are divided into modules [70]. Modules deal with the EMS functionality on a cell level and provide abstraction for a supervisory control. Communications are typically implemented using a fieldbus system, e.g., Controller Area Network (CAN), for automotive. HESSs, discussed in more detail in Section III, feature a power electronic converter and have a more complex topology compared with a battery or UC pack. The battery and the UC subsystem are typically well separated and can be treated individually by the battery management system (BMS) (with exception of managing the energy flow between the subsystems).

A. Protection

ESS store significant amounts of energy and require passive and active safety precautions to prevent an uncontrolled release. Although electromagnetically driven contactors are used as a form of last line of protection at the pack level, passive and active safety mechanisms within the pack are used to ensure the continued safe operation of the battery. Passive safety mechanisms are used to prevent worst case scenarios in case of electrical faults, high temperature, or high internal pressure [71]. Each cell is typically protected against overcurrents using positive temperature coefficient resettable fuses and short circuits using bimetallic circuit breakers [70]. Most battery cells also feature overpressure release valves. Modules are designed considering the expected physical abuse (vibration, impact, and so on) and thermal isolation of the cells, e.g., to prevent the progression of a thermal runaway [71].

EMSs are used to actively protect ESS. Battery and UC cells are designed to operate in a specified voltage and current range. Energy storage cells operate typically in the range $v_{\min} = 2.5$ V to $v_{\max} = 4.3$ V for Li-ion batteries [40], up to $v_{\max} = 2.7$ V for electrostatic double-layer capacitors [72], and $v_{\min} = 2.2$ V to $v_{\max} = 4$ V for hybrid UCs [73]. Cells are designed to handle a rated current but the minimum and maximum current depends on temperature. Electrostatic cells need to be derated when they find themselves above a certain temperature. The temperature dependence of electrochemical cells is nonlinear, e.g., Li-ion cells cannot be charged below a certain temperature.

Safe operation challenges arise when connecting cells in series (and parallel) to form a pack. Cells do not charge and discharge equally due to variations in intrinsic cell specifications, such as internal impedance and self-discharge rate. These variations are caused by manufacturing tolerances, cell degradation, and temperature variations across a pack [74]. The EMS has to monitor each cell individually. Each cell has to be operated strictly within its operation limits to avoid gradually damaging some of the cells. Operation of a battery pack without protecting each cell corresponds to a nearly exponential reduction of the battery life as the string length increases [75], [76]. In contrast to passive protections, fine-grained safety mechanisms can be implemented in the EMS, e.g., considering temperature-dependent current limits or communicate with chargers and loads to adjust the operation.

B. State and Parameter Estimation

Cells are characterized by the nominal capacity Q_n. It defines the amount of charge that a cell provides at a specified current and temperature. The effective capacity Q depends on the load current (C-rate) and is described by Peukert's law with $I^n t = \text{const.}$, where $n \in [1, 1.5]$ is a chemistry-dependent empirical factor [77], [78]. Although Peukert's equation performs well at room temperature, it does not consider different temperatures and battery aging [78]–[81]. In general, Q depends on temperature, whereby a decrease in temperature induces a reduction of Q [79]. For Li-ion cells, a decrease in temperature increases the cell impedance (increased electrolyte resistance and reduced mass transport) [79], [82]. Above nominal temperature, the capacity increases only by a limited amount (at increased cell corrosion and potential safety risks). Increase in cell impedance as well as loss of active mass are also a result of battery aging [83], [84], which has been found to increase capacity fade [85]–[87]. The SOC $x \in [0, 1]$ is the normalized charge of a cell and defines the amount of charge $q = Q\,x$ that is stored in a cell.

A modern EMS estimates the SOC of each cell in the pack [88], [89]. The SOC cannot be directly measured. The SOC is mapped onto the open circuit voltage (OCV) [90] and, in general, is a nonlinear function, varying with age and temperature [82], [91], [92]. In particular, this function is nonlinear in the case of batteries but is linear in nature for UCs. OCV-based SOC estimation measures the terminal voltage after a cell has rested for minutes or hours (dependent on chemistry) to attain electrochemical equilibrium and reconstructs SOC with lookup tables. The main limitations of this approach are that it cannot be used during operation; the OCV–SOC characteristic is subject to changes when a cell ages, and some battery chemistries (e.g., Li-ion) have flat voltage profiles for intermediate charge levels that yields large uncertainties in SOC estimation. The conceptually opposing approach is coulomb counting [82], [88], [93]–[97]. This method integrates the current flowing into or out of each battery cell. For chemistries with low self-discharge rates, such as Li-ion, this method can accurately determine small changes in the stored amount of charge. The main limitation

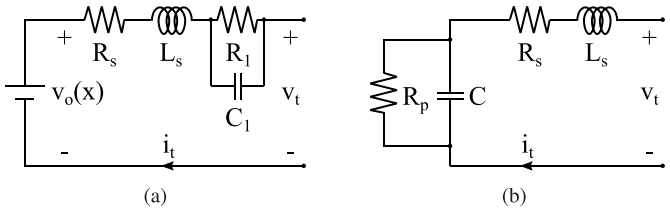

Fig. 2. Lumped parameter cell models with OCV $v_o(x)$, ESR R_s, equivalent series inductance L_s, self-discharge resistance R_p, and series RC element. (a) Battery model. (b) UC model.

of this approach is the capacity and charge, i.e., discharge efficiency needs to be known with sufficient precision. In addition, the method is susceptible to the drifts of the estimates over time due to small measurement or coefficient offsets. Hence, the SOC needs to be corrected, which is typically done through the OCV information [82], [88], [95], [96], [98]–[100]. More sophisticated methods have been developed to overcome the shortcomings of the above-mentioned techniques. These methods are based on (adaptive) cell models and use voltage and current measurements to correct the estimate. They can be classified with respect to their estimation principle: Luenberger observer [57], [88], [101]–[103], adaptive observer [88], [104], [105], sliding mode observer [57], [88], [100], [106]–[110], and Kalman Filters [2], [111]–[113].

Accurate SOC estimation requires cell models, e.g., lumped parameter models and electrochemical models [91], [92], [114]. Each model relies on experimental data to render accurate representations [2], [111], [112], [115]. Simple lumped parameter models for battery and supercapacitor cells are shown in Fig. 2 [82], [116]. Linear and nonlinear elements can be added to these models for higher accuracy or to model specific behavior [117], [118]. Electrochemical models offer higher fidelity than lumped parameter or equivalent circuit-based models; however, they tend to be much more computationally expensive. The latter ensues as a result of the extensive amount of parameter fitting involved in electrochemical models as opposed to lumped parameter and equivalent circuit models. The properties of UC and battery cells tend to change due to aging. Hence, it is beneficial to estimate the main parameters to improve the model accuracy [119], [120].

Parameter estimation typically focuses on the estimation of the capacity and/or the impedance [82], [88]. The capacity is estimated to improve the knowledge of the energy stored in cells, e.g., using the OCV–SOC relationship [121]–[125], augmented Kalman filters [126]–[128], or recursive least squares (RLS) filters [129], [130]. It is worth noting that the close relationship of SOC and capacity poses numerical and stability challenges for the estimation of both values [131]. The impedance is estimated to approximate losses during charging and discharging and predict the available power in the batteries [82], [88]. The impedance can be measured by impedance spectroscopy in laboratory conditions. Similar techniques can be employed using auxiliary circuits [132]–[134] or the impedance can be estimated, e.g., using Kalman filters [113], [135]–[141] or RLS filters [95], [98], [142]–[144]. The impedance in combination with current and voltage measurements can be used to predict the available power, named state of power [82], [88].

Parameter approximations can also be used to estimate the state of health (SOH). The fitness of a cell or pack for a specific application deteriorates over its lifetime due to aging [82], [88]. The SOH quantifies the condition of a module or cell compared with its ideal conditions at the time of manufacturing. It is a figure of merit that does not correspond to a physical entity and is given in per unit where 1 is the performance of a new cell (without manufacturer tolerances) and 0 indicates the minimum level that is acceptable for a certain application. If a pack reaches an SOH equal to zero, the pack needs to be replaced to ensure a minimum capability, e.g., the range of an EV. However, a pack with the same characteristics can be perfectly suitable for a less demanding application, e.g., as an energy storage element in a smart home, and batteries can be reused in what is known as the second-life operation [145].

SOH can be determined with respect to energy (SOH_E) or with respect to power (SOH_P). Both indices are calculated while considering one or more battery parameters [82], [88], [119], [120]. The main parameter for SOH_E computation is the capacity [119], [120] but it can also consider voltage and/or self-discharge rates [82], [88] to more accurately capture the energy capabilities. On the other hand, SOH_P is mainly determined based on the resistance or impedance [82], [88], where it is commonly referred to as SOH_R, and can consider further parameters. The SOH_P has priority in an HEV. In EVs, the ESS needs to ensure sufficient SOH_P and SOH_E to be able to meet the power and range requirements. SOH_P and SOH_E become important parameters when considering an HESS, which couples two or more storage devices together. This will be discussed in greater detail in Section IV. The SOH trend can also be extrapolated to estimate the remaining useful life (RUL) [82], [88] of a cell or pack to predict necessary maintenance. Alternatively, the RUL can be estimated based on observation of the battery conditions and a battery lifetime model [88].

C. Balancing and Redistribution

An unbalanced pack has a low effective capacity and runs an increased risk to charge/discharge the cells over/under the safe operating voltages. Thus, modern EMS uses the techniques to equalize the SOC of the cells. There are two classes of balancing hardware: dissipative and nondissipative. In dissipative balancing, excess charge is drawn from the cells with the highest SOC and is dissipated through a shunt resistor or transistor. Nondissipative hardware uses power electronics links, i.e., dc/dc converters, to move charge between cells [146]–[150]. Nondissipative hardware can be further distinguished from a functional point of view. Balancing refers to equalizing the cell SOCs in a string and is typically applied during charging. The useful capacity of a balanced string is that of its weakest cell. During discharge, operation has to stop once the weakest cell is empty even if the stronger cells still contain energy. Redistribution dynamically moves charge from the stronger cells to the weaker cells during operation, such that all of the energy stored in the stack can be used. It can

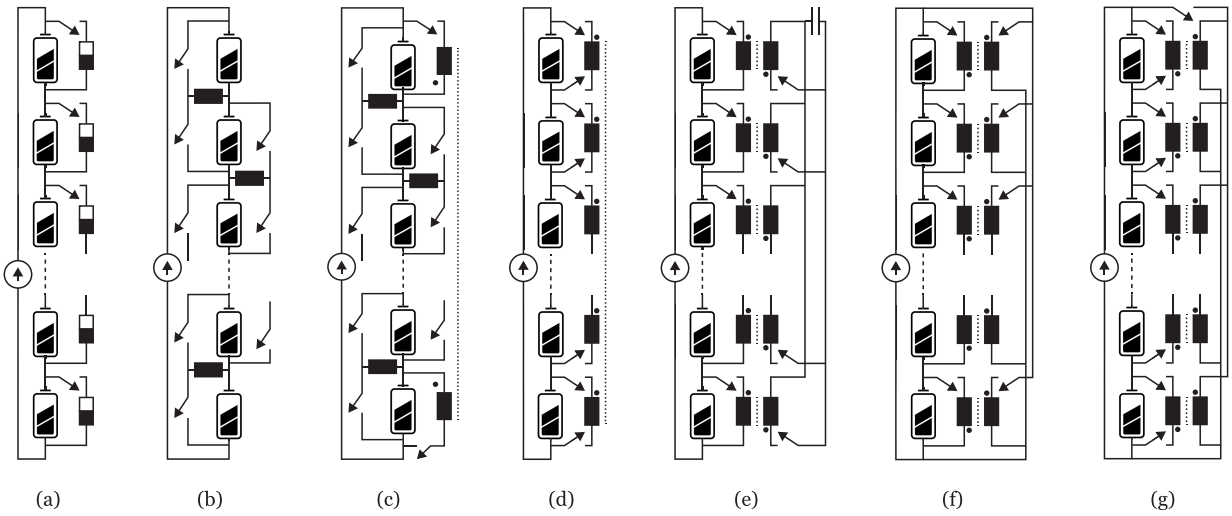

Fig. 3. Balancing topologies. (a) Dissipative. (b) Line. (c) Ring. (d) Inductive. (e) Capacitive. (f) Individual. (g) Common.

be regarded as a form of nondissipative balancing where each link is capable of handling the required power.

Dissipative balancing can be either passive and active. Passive balancing relies on system properties, i.e., the cell voltage, to achieve balanced cells. An example is a variant of the configuration shown in Fig. 3(a), which connects the shunt resistors permanently in parallel to the cells during balancing. Balancing is achieved, since a higher current is drawn from cells that have a higher cell voltage compared with cells with lower voltage. However, passive balancing draws charge from all cells, including the ones with low SOC (compared with other cells) and requires a significant amount of time for balancing. These drawbacks are addressed using active dissipative balancing that is obtained by combining the same topology with a control system that actively controls the balancing switches. The controller identifies cells with high SOC and removes excess charge from these cells dissipating the energy in a resistor. Nondissipative topologies move charge between battery cells. They are typically active and use a control strategy to identify the balancing current in the links. They can be classified into cell to cell, cell to stack, and stack to cell topologies. Power electronics converters are used to move charge across the stack and realize the balancing links. Examples are shown in Fig. 3.

The performance of SOC balancing hardware can be rated in terms of time to balance and energy loss to balance [151]. Time to balance defines how much time is required by a balancing topology to achieve a balanced SOC given a worst case initial unbalance and link current, i.e., power and rating. Energy loss to balance defines how much energy is dissipated in heat while balancing a worst case initial unbalance. The worst case initial unbalance of a topology is iterated over all admissible initial unbalances defined by a maximum unbalance in percentage [151]. In comparison, active dissipative balancing improves significantly over passive balancing in terms of both performance metrics, since the energy dissipation is selective and applied only to cells with excess charge. Also, active dissipative balancing can be regarded as benchmark reference in terms of t2b as it requires a constant time for all admissible initial unbalances. Some nondissipative topologies can match this t2b benchmark and reduce e2b significantly [151]. Examples are the capacitive storage element topology and the multiple inductor topology that are generally suitable for large battery stacks.

Active dissipative balancing is popular in demanding applications (e.g., HEV and EV), since the packs require monitoring of cell voltages, temperatures, and so on. Thus, the infrastructure for SOC estimation and balancing algorithms is available. Dissipative balancing is generally regarded as more cost effective than nondissipative balancing, since the latter one requires links with more elements, i.e., dc/dc converters [69]. However, nondissipative topologies simplify the cooling of battery packs as they reduce the waste heat generated within a battery pack. Also, their ability to implement the redistribution functionality allows to use the unbalanced energy of a battery stack that increases the battery life when some cells loose capacity.

IV. Hybrid Energy Storage Systems

As outlined earlier, there are no perfect energy storage devices, which perform ideally when considering factors, such as specific energy, specific power, affordability, and safety to name a few. Discharge/charge rates are slower in batteries, since charge transfer only occurs through reducing and oxidizing reactions. Thus, UCs have the power density to sustain the dynamic power profile of a vehicle but they do not have the energy density to propel the vehicle for a sufficiently long electric-only driving range. UCs have an almost quasi-infinite cycle life relative to Li-ion batteries, since operationally they lack the chemical reactions contributing to battery cell degradation [61], [152]. Two or more devices can be coupled to obtain an HESS, which combines the benefits of the various available ESSs. Any combination of battery systems, UCs, fuel cells, or flywheels can be considered for an HESS [60], [153]. UCs can be combined with a fuel cell device in a HESS to mitigate the slow dynamic response rate of current fuel cell technology [154], [155]. Flywheels and batteries have also been coupled in an HESS where peak demand is offset to the more power dense flywheel [156], [157]. One recent

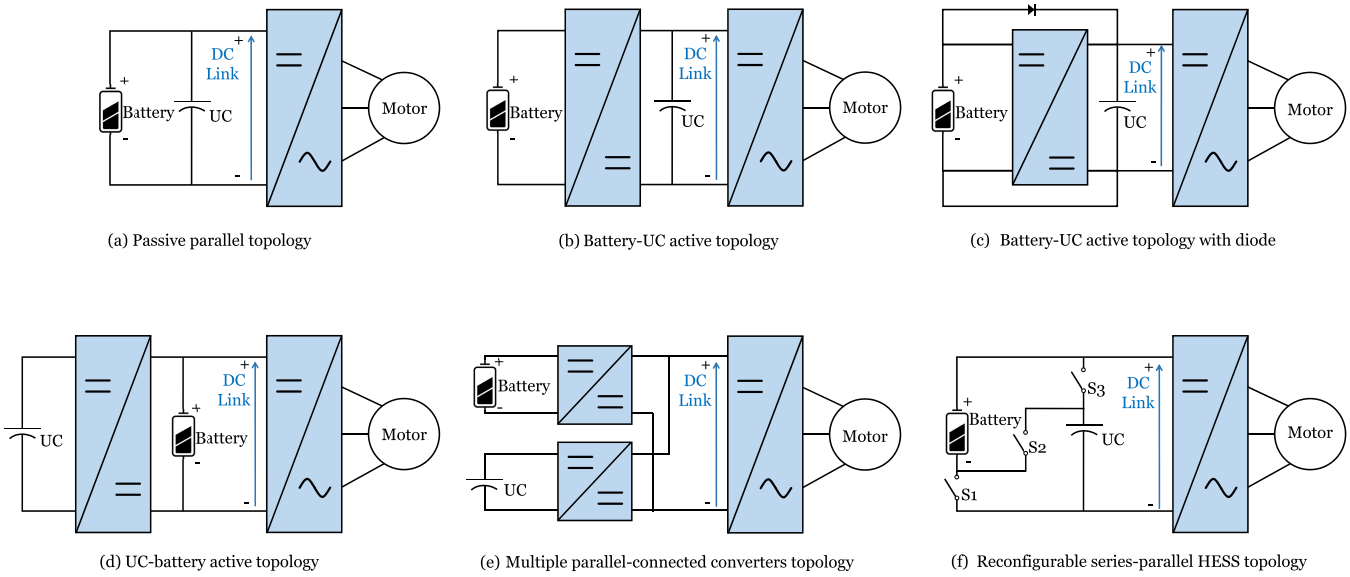

(a) Passive parallel topology (b) Battery-UC active topology (c) Battery-UC active topology with diode

(d) UC-battery active topology (e) Multiple parallel-connected converters topology (f) Reconfigurable series-parallel HESS topology

Fig. 4. Prominent HESS topologies. In (a), there are no power converters used and that is why this topology is called a passive parallel configuration. Power electronics are used to interface a battery pack to a UC bank in (b)–(f). These are referred to as active topologies, each one having its respective benefits and drawbacks.

study proposed the cell level coupling of a battery and UC in what they define as a hybrid cell [158]. HESSs are also extensively researched for distributed generation in microgrid systems. These have included the coupling of two or more renewable energy sources, such as photovoltaic systems, tidal energy generators, wind turbine generators, fuel cell systems, and battery systems to name a few [159]–[162].

For automotive applications, studies have found that interfacing a UC bank with a battery pack can have significant improvements on the driving range of electric drive vehicles [163]–[166]. One study using a fuzzy sliding mode controller on a battery/UC HESS showed the most promise, stating an improvement in a driving range of $>30\%$ [164]. In addition, the cost of a battery pack in an EV and a PHEV is by far the most costly component of the vehicle. Thus, combining a UC bank with a battery pack offers manufacturers the option of reducing the size and, therefore, the cost of the battery pack. Some notable HESS used in prototypes include the combination of lead-acid batteries with NiMH, Li-ion, or UCs in microhybrids [42]. In addition, lead-acid [60], [152] and ZEBRA batteries [6], [167]–[169] have also been buffered with UCs to increase power and battery life in EVs.

Another prominent benefit of an HESS is its ability to protect battery SOH and, in turn, prolong battery lifetime. In effect, offsetting the peak load demand at the dc link onto the UC allows the battery to provide a mostly constant load profile. As discussed earlier, imposing peak load demands on Li-ion batteries increases battery wear, which describes an increase in deposits at the battery's solid-electrolyte interface (SEI) [158]. The latter is described as one of the more prevalent factors leading to battery aging [83], [87], [158], [170]–[173]. A recent study investigates Li-ion battery aging through the growth of the SEI in the battery of an HESS using physics-based battery models [158]. For EVs, coupling a battery and a UC in an HESS, $\mathrm{SOH_E}$ is calculated based on the battery as the UC stores a limited amount of energy. Similarly, the calculation of $\mathrm{SOH_P}$ is mainly based on the UC, since this is used to provide peak power. Compared with a battery-based ESS, an HESS has the potential to significantly reduce SOH deterioration and improve battery lifetime [158], [174], [175]. $\mathrm{SOH_P}$ given by the UCs can be regarded as nearly constant due to their high cycle life and they can shield the battery from peak power demands and microcycles, which limits the deterioration of $\mathrm{SOH_E}$ [116]. Typically, research has focused on modeling aging effects of the battery [158], [174], [175], since the cycle lifes of batteries are the orders of magnitude smaller than the cycle lifes of UCs.

The battery and the UC are usually modeled separately using methods discussed in Section III, such as equivalent circuit models [116], [152], [176]–[178] or electrochemical models [158]. SOC is estimated for both storage devices separately using methods discussed in Section III, such as Coulomb counting [116], [152], [176], [177]. Depending on the configuration of the HESS under consideration, these two models can be interfaced with power electronics models or a power balancing function to mimic the exchange of energy between both sources performed by a power converter [116], [176], [177].

HESS systems are classified under two major types of classes: passive HESS systems, which do not require power converters and active configurations, which require dc/dc converters. In Section IV-A, some predominant battery-UC HESS configurations for automotive applications will be reviewed and are shown in Fig. 4.

A. Passive Parallel Connection

In this topology, also called passive shunt connection, shown in Fig. 4(a), the UC bank is directly connected to the

battery bank. The current output from both energy sources is highly dependent on their internal *RC* values [179], [180] given the lack of dc/dc converter. Since impedance is typically lower for UCs, energy will preferentially flow out of the UC bank when large burst of power is requested. The advantages in this configuration lie in the lack of power converter, which makes for a smaller, lighter, and more affordable HESS. In addition, the fluctuations in the dc link voltage are much smaller when the battery is locked on to the dc bus.

In this configuration, the UC bank is acting as a low-pass filter, which attenuates high peaks and low troughs. Since the UC is locked to the voltage of the battery pack, the UC must be sized accordingly. Typically, this size is larger than is required to gain the convenience of the low-pass filter characteristics [181]. The terminal voltage at the output of the HESS will follow the battery's discharge curve, which can fluctuate considerably between the battery pack's fully charged state and the fully discharged state. Another disadvantage of having the UC voltage locked to the voltage of the battery pack is that the usable voltage range of the UC is reduced, and therefore, the power being outputted by the UC is limited [179]–[181]. Furthermore, as soon as the UC delivers current to the load, its voltage will drop, at which point the battery begins to supply current to recharge the UC as well as to supply the load. Therefore, the battery must either be able to supply the rated power of the electric drive powertrain or the controls system must not permit the battery to supply more than its rated power. This is essentially an *RC* circuit where the charge/discharge current is solely dependent on the battery/UC parameters. Although, the passive parallel configuration is simple, light, less costly, and offers no additional complexity of power electronics and their controls systems, it compromises on performance and exposes the battery to peak power demand [182].

B. Shunt Connection or Parallel Connection Through a DC/DC Converter

The optimal use of a UC bank requires interfacing the battery bank with the UC bank through a dc/dc converter. As mentioned earlier, ideally, a constant battery power output is preferred, since highly dynamic battery current profiles observed during highly volatile drive cycles could increase battery wear and degradation. Also, since UCs are much more robust and have much higher cycle life, it would be beneficial to offset the high bursts of power almost entirely onto the UCs during regenerative breaking and periods of acceleration.

1) Battery/UC Configuration: In this type of active parallel connection, shown in Fig. 4(b), the battery pack is connected through the dc/dc converter to the UC bank. This topology allows for a battery pack to be decoupled from the dc bus, therefore, allowing the pack to have a lower terminal voltage. Lower voltage and, hence, smaller battery packs are preferred, since they are lighter and less costly [181]. In this configuration, the UC bank is directly connected to the dc link; thus, the UC acts like a low-pass filter [183]. Although the UCs act as a low-pass filter, the entire range of the UC's voltage can be utilized, since the UC is not clamped directly to the battery [181]. For example, in the case of regenerative braking, keeping the UC bank at a low voltage relative to the battery voltage will allow most of the energy to naturally flow back into the UCs. This will also increase the efficiency of the system, since the UC pack typically has a smaller equivalent series resistance (ESR) [61], [72], [182] than the battery pack, and they can accept most of the power spikes experienced during regenerative braking. In addition, discharge and charge rates of the battery and UC packs can be controlled through the use of a power converter [2], [179]. Allowing the power converter to make decisions regarding the most opportune moments to buffer the energy in the UC versus the battery pack, and the rates at which the battery and UC can be discharged/charged can have a significant impact on the efficiency of the system as well as on the longevity of the battery lifetime [116]. Nevertheless, the added complexity of the power converter's control system can be a disadvantage of this configuration [179], [184].

A new variant of the active battery/UC configuration has emerged recently and is shown in Fig. 4(c) [185]. Through the external circuit includes a diode, the dc/dc converter can be bypassed when transferring energy from the battery to the dc link. The battery will charge the UC when the UC voltage is below than that of the battery. The battery can then be used to supply the average moving power, which the authors of this paper claim to be typically 10% of the peak power [183], [185]. Therefore, the dc/dc converter can be sized to be smaller in this topology than the power converter found in the previous active battery/UC configuration.

2) UC/Battery Configuration: In this type of active parallel connection, the UC is placed behind the dc/dc converter, as shown in Fig. 4(d). Decoupling the UC from the dc bus through the use of a dc/dc converter is desired in applications where a smaller UC pack is preferred [183]. The advantage of this topology is that it allows full utilization of the UC voltage range by controlling the dc/dc converter [186]. In addition, connecting the battery directly to the dc bus maintains a stable dc link voltage. The drawback, however, is seen when we look at large power burst scenarios where the amount of current flowing into or out of the battery cannot be fully controlled. In this type of scenario, it is preferable to connect the UC directly to the dc link, since it is better at accepting large pulses of energy. A less obvious but important drawback pertains to the power rating of the dc/dc converter. Since the UC bank will be supplying the large power spikes experienced by the vehicle during vigorous driving scenarios, the power converter will have to be rated for much higher powers and, therefore, must be sized to be much larger in this topology [187] than the converters used in the active battery/UC configuration.

C. Multiple Parallel-Connected Converters Configuration

Both the battery pack and the UC bank can be decoupled from the dc bus by interfacing each of them to a dc/dc converter. The outputs of the dc/dc converters are connected in parallel, as shown in Fig. 4(e). Since the voltages and the power flow of the two energy sources are also decoupled from each other, this configuration allows for independent

control of both UC and battery. A major advantage of this system is that it can allow for both the battery pack and the UC bank to have lower voltages than the dc link [183], which can vastly reduce the cost and size of the two energy sources. Since the UC pack and the battery pack are decoupled from the dc bus, this configuration couples the benefits of the active topologies mentioned above. In particular, this configuration maximizes the operational voltage range of the UC while maintaining a stable dc link [186]. Reliability is increased in this system, since power can continue to be provided to the dc link even if one of the storage devices fails, which serves as a great redundancy strategy [69]. It becomes clear, however, that the main drawbacks of this active topology are the added complexity of the control system, the larger size required for two power converters, and the additional cost incurred for the additional power electronics [179].

D. Series–Parallel Reconfigurable Hybrid Energy Storage System

A recent innovative HESS topology has been proposed and is shown in Fig. 4(f) [188]. This configuration utilizes various bidirectional switches to reconfigure the HESS from a series connection to a parallel connection. In a parallel configuration, a lower dc bus voltage is observed, which allows the battery pack to recharge the UC bank. This functionality is useful when the vehicle is in standstill operation. In addition, this configuration is most beneficial during peak demand, which typically occurs during the periods of acceleration or during regenerative breaking. If switch S2 is closed, then the UC bank is connected in series to the battery pack. This configuration can be useful if a dc bus voltage is required to be equal or higher than the UC voltage. In most cases, this will allow the electric motors to sustain peak torque at higher operating speeds. The addition of a power converter to this topology would allow either the UC or the battery to be decoupled form the dc link, affording this HESS configuration the same benefits enjoyed by the active battery/UC and UC/Battery topologies [188]. The drawback of such a configuration is of course the complexity of the controls. However, another potential and less obvious drawback would be the risks associated with the potential failure modes of switches S1, S2, and S3. Literature on this topology does not specify the nature of these switches, which are placed along the two dc links of the system. These dc links are designed to handle hundreds of volts and amperes. The use of conventional eletromagnetically driven contactors, which are known to have the possibility of contacts welding as a failure mode, can compromise the system. Solid state switches would add to the complexity of the controls but they are safer in this type of application, since they eliminate the risk of contact welding.

E. ESS and HESS Summary

Most prominent conventional batteries used in XEVs have been described in Section I, and a Ragone plot shown in Fig. 5 summarizes the specific energy as a function of the specific power of all the cell technologies considered in this paper. Lead-acid batteries are extensively used and will continue to be

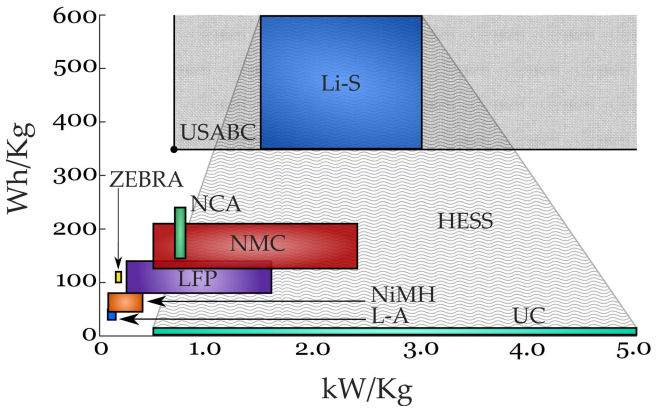

Fig. 5. Ragone plot of specific energy as a function of specific power. L-A, NiMH, LFP, NMC, NCA, and Li–S refer to Lead-acid, nickel–metal hydride, LiFePO, LiNiMnCo, LiNiCoAlO, and lithium–sulfur battery technologies, respectively. The performance of a next generation HESS coupling Li–S cells with UC cells is also shown.

used for vehicle low voltage systems due to the maturity of the technology; however, they lack most performance metrics to be useful for traction-type applications in XEVs. NiMH batteries generally have double the specific energy as well as better specific power than lead-acid technology and, therefore, have found widespread use in HEVs and some PHEVs. ZEBRA batteries are suitable for PHEV-type applications due to their high specific energy, which is comparable in value to LiFePO technology and a multiple of two to three times larger than that of NiMH. They also have a minimum cycle life of 2500 cycles, which exceeds any electrochemical storage device considered in this paper. However, their high self-discharge rate, which is an order of magnitude larger than the other electrochemical storage devices, put this technology at a disadvantage. Among the Li-ion cells considered in Section I, LiFePO cells typically have the lowest specific energy but can have a specific power that is higher than most. This makes them a suitable candidate for all types of XEV applications. In addition, their higher thermal runaway onset temperature makes them a safer choice for use in vehicles. The LiNiMnCo (NMC) and $LiNiCoAlO_2$ (NCA) cells have the highest specific energy of any readily available batteries. NCA cells can have a slightly larger specific energy than NMC cells, which generally have a much larger specific power. In either case, these superior performance metrics makes these cells great candidates for use in long range EVs. However, the lower thermal runaway onset temperature of these cells can add to the complexity of their management systems.

Prominent HESS configuration has been discussed earlier. The topology that is simplest, lightest, and least complex to control is clearly the passive parallel configuration. However, the lack in performance due to the UC being directly clamped to the battery pack and the lack of controllability are the shortcomings of such a system. The active configurations shown in Fig. 4(b)–(e) allow either the battery, the UC, or both energy sources to be decoupled from the dc link. This offers the advantage of controllibity. By decoupling the battery from the dc bus in the active battery/UC configuration,

shown in Fig. 4(b) and (c), the battery is protected from peak load demand, and a smaller and less costly battery pack can be used. The same advantages can be said for the UC in the active UC/battery topology, shown in Fig. 4(d). However, in this case, the battery becomes exposed to the peak load demand at the dc bus, and the much higher charge/discharge capabilities of the UC require a larger power converter. The multiple parallel-connected converters topology allows for complete control over both energy sources and, since they are both decoupled from the dc link, the sources can be both sized to be smaller. Complexity of controls can be a disadvantage in this configuration. Finally, the series–parallel reconfigurable HESS topology is not typical, in that it offers new beneficial functionalities, which the other active configurations do not offer. In particular, it can be reconfigured to have the two energy sources to be either in series or in parallel. These series/parallel modes can be selected according to which dc bus voltage offers the best performance and efficiency at different vehicle operating conditions. The control complexity of this system can also be a drawback. It becomes clear that the various HESS topologies each have their own benefits and disadvantages. In general, simplicity, no power electronics, affordability, and smaller size comes at the cost of performance while better performance comes at the price of control complexity, added size, weight, and cost. In essence, the best HESS topology is difficult to assess, however, each HESS configuration can be found to be better suited for a particular set of vehicle requirements.

F. Next Generation HESS and Future Direction

Although an HESS coupling conventional Li-ion battery cells with UC cells is capable of outperforming any single ESS technology, it will still fall short of the USABC goals for 2020. This becomes obvious when the reader attempts to combine the specifications of any of the Li-ion technologies shown in Fig. 1 with the specifications of UCs in a way, which maximizes the overall system performance. Certain metrics, such as a specific energy of 350 Wh/Kg, is currently unattainable, considering that the most energy dense Li-ion cells, which are commercially available today, are rated at 240 Wh/Kg. On the other hand, the first readily available Li–S cells are rated at 350 Wh/Kg; however, presently, this technology suffers from poor cycle life as can be seen in Fig. 1(g) and Table II. Therefore, the next generation HESS must invariably be composed of not only two energy sources but two energy sources intrinsically designed and manufactured to span different halves of the augmented USABC spider plot to meet the 2020 goals. If cell manufacturers can focus more of their efforts on producing cathode and electrolyte materials, which would allow the battery cells to better dominate certain performance metrics over others, then a combination of ESS technologies in an HESS has the possibility to match and exceed most, if not all, the USABC goals.

One might argue that cell cost can still remain to be a significant challenge in an HESS as it is with conventional ESS. However, a recent study, showing that battery cell cost is dropping faster than previously predicted [22], shows that the USABC goal for cell cost can be reached. It is anticipated that cell cost will be further reduced by 15–20% by 2017 due to projects, such as Tesla's Gigafactory, which is increasing the scale of production infrastructure to drive down manufacturing costs of battery cells [42].

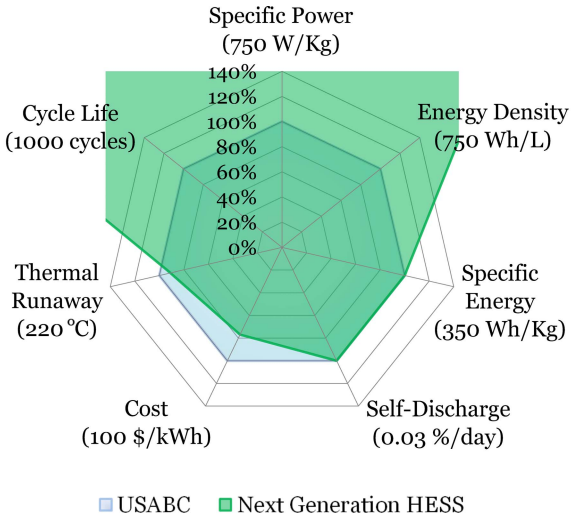

Fig. 6. Performance of next generation HESS neglecting electronics.

The greatest advantages offered by HESS are their higher power density, prolonged battery cycle life, and extension of driving range. These benefits can still be reaped while maintaining relatively low production costs if an HESS topology, such as the active battery/UC topology with a diode or the passive parallel configuration, is chosen. The latter two HESS configurations have the possibility of being more affordable, since they require little to no power electronics, respectively.

Although Li–S cells still have obvious challenges, which need to be mitigated before, they can be used in mainstream commercial applications; a combination of the latter with UCs has the possibility of reaching most of the augmented USABC goals in a next generation HESS. The Ragone plot shown in Fig. 5 compares the performance of such an HESS with other prominent traditional battery technologies considered in Section I. The area characterizing the HESS performance in this plot neglects the weight of power electronics, which might be used to interface the two storage devices. A next generation HESS can utilize a technology, such as Li–S, since it meets some of the augmented USABC 2020 goals, such as specific energy, energy density, and estimated cost, and has a sufficiently high thermal runaway onset temperature. Conventional UCs or hybrid UCs can meet other USABC goals, such as specific power and cycle life. The maximum performance, which can be achieved in such a system, is shown in Fig. 6 and almost spans the full breadth of the USABC spider plot. This plot is based on the upper limit of what a potential system can attain in terms of performance. In the case of specific energy, energy density, and specific power, a passive parallel HESS topology is considered whereby no power electronics are required. Since Li–S cells are still not widely available commercially, manufacturers can still reap the benefits of HESS with cell technologies available today. If an HESS is chosen over conventional ESS, battery cell lifetimes can be

extended, which, therefore, extends the lifetime of XEVs and increases costumer satisfaction [116], [158]. This is in addition to other advantages mentioned earlier, such as higher specific power.

In the final analysis, looking ahead, better ESS performance, better efficiency, and longevity of battery life will, unavoidable, become increasingly important as the XEV market grows. In such a case, research efforts should not only be focused on developing better performing battery cells but on a better marriage between various readily available energy storage devices and power electronics. Li-ion battery technology is currently the mainstream mass produced battery chemistry used in long range electric drive vehicles. The battery community is placing a considerable amount of research efforts and resources in the development of the next incumbent battery technology. However, HESSs have the capability to improve performance and efficiency, no matter the battery technology used within it. To that end, considerably more resources should be allocated to developing simpler, smaller, and more affordable HESSs, which can be better suited for mass production.

V. Conclusion

Alternative energy vehicles are gaining market acceptance and a race to a cost competitive ESS solution is taking place among leading vehicle manufacturers. There exist many battery and UC technologies that can meet the demand of the various flavors of XEV. An overview of readily available battery and UC technologies is given along with a description of current advances in Li-based battery technologies. BMSs and battery pack design are also reviewed. Conventional protection mechanisms, such as under/over voltage, over charge/discharge, and over-temperature protection schemes, were discussed. Battery and UC cell models, state, and parameter estimation as well as cell balancing and redistribution are also reviewed. HESS topologies found in the literature were discussed where the benefits as well as the drawbacks of each configuration were discussed. Finally, an assessment of how HESS compares to current electrochemical and electrostatic storage devices as well as how they can fit into the modern landscape of electric drive vehicles is performed. In this assessment, coupling UCs with Li–S cell technology was investigated as an example of the next generation HESS that can meet the augmented USABC 2020 goals almost entirely. While the research community mitigates many shortcomings of commercial and prototypical ESS technologies, HESSs through their superior performance have the ability to increase driving range, increase the electric drive's specific power, and prolong battery lifetimes. Looking forward, a greater collaboration between the research community, cell manufacturers, and vehicle manufacturers can lend to various types of battery cells produced to dominate certain performance metrics. Moreover, additional research efforts to create a better marriage between battery/UC technologies and power electronics can spawn new, innovative, and affordable HESS topologies, which improve upon traditional ESS technology.

References

[1] *Energy Technology Perspective 2008*, Int. Energy Agency, Paris, France, 2008.

[2] A. Emadi, *Advanced Electric Drive Vehicles*. New York, NY, USA: CRC Press, 2015.

[3] B. Bilgin *et al.*, "Making the case for electrified transportation," *IEEE Trans. Transport. Electrific.*, vol. 1, no. 1, pp. 4–17, Jun. 2015.

[4] N. Omar *et al.*, "Rechargeable energy storage systems for plug-in hybrid electric vehicles—Assessment of electrical characteristics," *Energies*, vol. 5, no. 12, pp. 2952–2988, 2012.

[5] J. L. Sudworth, "The sodium/nickel chloride (ZEBRA) battery," *J. Power Sour.*, vol. 100, nos. 1–2, pp. 149–163, 2001.

[6] J. Dixon, I. Nakashima, E. F. Arcos, and M. Ortuzar, "Electric vehicle using a combination of ultracapacitors and ZEBRA battery," *IEEE Trans. Ind. Electron.*, vol. 57, no. 3, pp. 943–949, Mar. 2010.

[7] H. Chen, T. N. Cong, W. Yang, C. Tan, Y. Li, and Y. Ding, "Progress in electrical energy storage system: A critical review," *Prog. Natural Sci.*, vol. 19, no. 3, pp. 291–312, 2009.

[8] S. Sabihuddin, A. E. Kiprakis, and M. Mueller, "A numerical and graphical review of energy storage technologies," *Energies*, vol. 8, no. 1, pp. 172–216, 2014.

[9] T.-K. Ying, X.-P. Gao, W.-K. Hu, F. Wu, and D. Noréus, "Studies on rechargeable NiMH batteries," *Int. J. Hydrogen Energy*, vol. 31, no. 4, pp. 525–530, 2006.

[10] P. Albertus, J. Christensen, and J. Newman, "Modeling side reactions and nonisothermal effects in nickel metal-hydride batteries," *J. Electrochem. Soc.*, vol. 155, no. 1, pp. A48–A60, 2008.

[11] W. Kempton and T. Kubo, "Electric-drive vehicles for peak power in Japan," *Energy Policy*, vol. 28, no. 1, pp. 9–18, 2000.

[12] P. Bäuerlein, C. Antonius, J. Löffler, and J. Kümpers, "Progress in high-power nickel–metal hydride batteries," *J. Power Sour.*, vol. 176, no. 2, pp. 547–554, 2008.

[13] F. Torabi and V. Esfahanian, "Study of thermal-runaway in batteries: II. The main sources of heat generation in lead-acid batteries," *J. Electrochem. Soc.*, vol. 160, no. 2, pp. A223–A234, 2012.

[14] D. Pavlov, "Energy balance of the closed oxygen cycle and processes causing thermal runaway in valve-regulated lead/acid batteries," *J. Power Sour.*, vol. 64, nos. 1–2, pp. 131–137, 1997.

[15] P. H. Smith, T. N. Tran, T. L. Jiang, and J. Chung, "Lithium-ion capacitors: Electrochemical performance and thermal behavior," *J. Power Sour.*, vol. 243, pp. 982–992, Dec. 2013.

[16] G. Mulder *et al.*, "Comparison of commercial battery cells in relation to material properties," *Electrochim. Acta*, vol. 87, pp. 473–488, Jan. 2013.

[17] Y. V. Mikhaylik, I. Kovalev, R. Schock, K. Kumaresan, J. Xu, and J. Affinito, "High energy rechargeable Li-S cells for EV application: Status, remaining problems and solutions," *ECS Trans.*, vol. 25, no. 35, pp. 23–34, 2010.

[18] *Advanced Battery Development—2013 Annual Progress Report*, U.S. Dept. Energy, Washington, DC, USA, 2013.

[19] M. Hagen, D. Hanselmann, K. Ahlbrecht, R. Maça, D. Gerber, and J. Tübke, "Lithium–sulfur cells: The gap between the state-of-the-art and the requirements for high energy battery cells," *Adv. Energy Mater.*, vol. 5, no. 16, 2015.

[20] H. Popp, J. Attia, F. Delcorso, and A. Trifonova, "Lifetime analysis of four different lithium ion batteries for (plug-in) electric vehicle," in *Proc. Transp. Res. Arena*, Paris, France, 2014.

[21] W.-T. Xu, H.-J. Peng, J.-Q. Huang, C.-Z. Zhao, X.-B. Cheng, and Q. Zhang, "Towards stable lithium–sulfur batteries with a low self-discharge rate: Ion diffusion modulation and anode protection," *ChemSusChem*, vol. 8, no. 17, pp. 2892–2901, 2015.

[22] B. Nykvist and M. Nilsson, "Rapidly falling costs of battery packs for electric vehicles," *Nature Climate Change*, vol. 5, no. 4, pp. 329–332, 2015.

[23] F. Xu *et al.*, "Failure investigation of $LiFePO_4$ cells under overcharge conditions," *J. Electrochem. Soc.*, vol. 159, no. 5, pp. A678–A687, 2012.

[24] A. W. Golubkov *et al.*, "Thermal-runaway experiments on consumer Li-ion batteries with metal-oxide and olivin-type cathodes," *RSC Adv.*, vol. 4, no. 7, pp. 3633–3642, 2014.

[25] A. W. Golubkov *et al.*, "Thermal runaway of commercial 18650 Li-ion batteries with LFP and NCA cathodes—Impact of state of charge and overcharge," *RSC Adv.*, vol. 5, no. 70, pp. 57171–57186, 2015.

[26] J. Seo, S. Sankarasubramanian, C.-S. Kim, P. Hovington, J. Prakash, and K. Zaghib, "Thermal characterization of Li/sulfur, Li/S–$LiFePO_4$ and Li/S–LiV_3O_8 cells using isothermal micro-calorimetry and accelerating rate calorimetry," *J. Power Sour.*, vol. 289, pp. 1–7, Sep. 2015.

[27] H. A. Catherino, "Complexity in battery systems: Thermal runaway in VRLA batteries," *J. Power Sour.*, vol. 158, no. 2, pp. 977–986, 2006.

[28] M. Takahashi, K. Komatsu, and K. Maeda, "The safety evaluation test of lithium-ion batteries in vehicles—Investigation of overcharge test method," *ECS Trans.*, vol. 41, no. 39, pp. 27–41, 2012.

[29] Q. Wang, P. Ping, X. Zhao, G. Chu, J. Sun, and C. Chen, "Thermal runaway caused fire and explosion of lithium ion battery," *J. Power Sour.*, vol. 208, pp. 210–224, Jun. 2012.

[30] C.-Y. Wen, C.-Y. Jhu, Y.-W. Wang, C.-C. Chiang, and C.-M. Shu, "Thermal runaway features of 18650 lithium-ion batteries for $LiFePO_4$ cathode material by DSC and VSP2," *J. Thermal Anal. Calorimetry*, vol. 109, no. 3, pp. 1297–1302, 2012.

[31] K. Yeow and H. Teng, "Characterizing thermal runaway of lithium-ion cells in a battery system using finite element analysis approach," *SAE Int. J. Alt. Power.*, vol. 2, no. 1, pp. 179–186, 2013.

[32] T. J. Knipe, L. Gaillac, and J. Argueta, "100,000-mile evaluation of the Toyota RAV4 EV," Southern California Edison, Electr. Vehicle Tech. Center, Rosemead, CA, USA, Tech. Rep., 2003, pp. 1–12.

[33] T. B. Reddy, *Linden's Handbook of Batteries*, 4th ed. New York, NY, USA: McGraw-Hill, 2010, ch. 22.

[34] D. A. Wetz, P. M. Novak, B. Shrestha, J. Heinzel, and S. T. Donahue, "Electrochemical energy storage devices in pulsed power," *IEEE Trans. Plasma Sci.*, vol. 42, no. 10, pp. 3034–3042, Oct. 2014.

[35] C.-H. Dustmann, "Advances in ZEBRA batteries," *J. Power Sour.*, vol. 127, nos. 1–2, pp. 85–92, 2004.

[36] K. B. Hueso, M. Armand, and T. Rojo, "High temperature sodium batteries: Status, challenges and future trends," *Energy Environ. Sci.*, vol. 6, no. 3, pp. 734–749, 2013.

[37] M. R. Palacín, "Recent advances in rechargeable battery materials: A chemist's perspective," *Chem. Soc. Rev.*, vol. 38, no. 9, pp. 2565–2575, 2009.

[38] I. J. Fernández, C. F. Calvillo, A. Sánchez-Miralles, and J. Boal, "Capacity fade and aging models for electric batteries and optimal charging strategy for electric vehicles," *Energy*, vol. 60, pp. 35–43, Oct. 2013.

[39] T. B. Reddy, *Linden's Handbook of Batteries*, 4th ed. New York, NY, USA: McGraw-Hill, 2010, ch. 26.

[40] Panasonic. (2012). *Panasonic Lithium Ion NCR18650 Specifications Version 13.11 R1*. [Online]. Available: http://industrial.panasonic.com/cdbs/www-data/pdf2/ACA4000/ACA4000CE240%.pdf

[41] Y. Su, S. Cui, Z. Zhuo, W. Yang, X. Wang, and F. Pan, "Enhancing the high-voltage cycling performance of $LiNi_{0.5}Mn_{0.3}Co_{0.2}O_2$ by retarding its interfacial reaction with an electrolyte by atomic-layer-deposited Al_2O_3," *ACS Appl. Mater. Interfaces*, vol. 7, no. 45, pp. 25105–25112, 2015.

[42] M. Anderman, "Assessing the future of hybrid and electric vehicles: The xEV industry insider report," Advanced Automotive Batteries, Tech. Rep., 2013.

[43] M. Barghamadi, A. Kapoor, and C. Wen, "A review on Li-S batteries as a high efficiency rechargeable lithium battery," *J. Electrochem. Soc.*, vol. 160, no. 8, pp. A1256–A1263, 2013.

[44] P. G. Bruce, S. A. Freunberger, L. J. Hardwick, and J.-M. Tarascon, "Li–O2 and Li–S batteries with high energy storage," *Nature Mater.*, vol. 11, no. 1, pp. 19–29, 2012.

[45] P. G. Bruce, L. J. Hardwick, and K. M. Abraham, "Lithium-air and lithium-sulfur batteries," *MRS Bull.*, vol. 36, no. 7, pp. 506–512, 2011.

[46] L. Chen and L. L. Shaw, "Recent advances in lithium–sulfur batteries," *J. Power Sour.*, vol. 267, pp. 770–783, Dec. 2014.

[47] F. Mizuno, S. Nakanishi, Y. Kotani, S. Yokoishi, and H. Iba, "Rechargeable Li-air batteries with carbonate-based liquid electrolytes," *Electrochemistry*, vol. 78, no. 5, pp. 403–405, 2010.

[48] A. Kraytsberg and Y. Ein-Eli, "Review on Li–air batteries—Opportunities, limitations and perspective," *J. Power Sour.*, vol. 196, no. 3, pp. 886–893, 2011.

[49] P. Johansson and R. Dominko, "EUROLIS—European lithium sulphur cells for automotive applications," in *Proc. EVS27 Symp.*, Nov. 2013, pp. 1–3.

[50] X. Ji and L. F. Nazar, "Advances in Li–S batteries," *J. Mater. Chem.*, vol. 20, no. 44, pp. 9821–9826, 2010.

[51] H. Wang *et al.*, "Graphene-wrapped sulfur particles as a rechargeable lithium–sulfur battery cathode material with high capacity and cycling stability," *Nano Lett.*, vol. 11, no. 7, pp. 2644–2647, 2011.

[52] S. Lu, Y. Cheng, X. Wu, and J. Liu, "Significantly improved long-cycle stability in high-rate Li–S batteries enabled by coaxial graphene wrapping over sulfur-coated carbon nanofibers," *Nano Lett.*, vol. 13, no. 6, pp. 2485–2489, 2013.

[53] R. Chen *et al.*, "Graphene-based three-dimensional hierarchical sandwich-type architecture for high-performance Li/S batteries," *Nano Lett.*, vol. 13, no. 10, pp. 4642–4649, 2013.

[54] M.-Q. Zhao *et al.*, "Graphene/single-walled carbon nanotube hybrids: One-step catalytic growth and applications for high-rate Li–S batteries," *ACS Nano*, vol. 6, no. 12, pp. 10759–10769, 2012.

[55] S. Evers and L. F. Nazar, "Graphene-enveloped sulfur in a one pot reaction: A cathode with good coulombic efficiency and high practical sulfur content," *Chem. Commun. (Camb)*, vol. 48, no. 9, pp. 1233–1235, 2012.

[56] N. Liu, L. Hu, M. T. McDowell, A. Jackson, and Y. Cui, "Prelithiated silicon nanowires as an anode for lithium ion batteries," *ACS Nano*, vol. 5, no. 8, pp. 6487–6493, 2011.

[57] X. Chen, W. Shen, Z. Cao, and A. Kapoor, "A comparative study of observer design techniques for state of charge estimation in electric vehicles," in *Proc. 7th IEEE Conf. Ind. Electron. Appl. (ICIEA)*, Jul. 2012, pp. 102–107.

[58] D. S. Jung, T. H. Hwang, S. B. Park, and J. W. Choi, "Spray drying method for large-scale and high-performance silicon negative electrodes in Li-ion batteries," *Nano Lett.*, vol. 13, no. 5, pp. 2092–2097, 2013.

[59] N. Liu *et al.*, "A pomegranate-inspired nanoscale design for large-volume-change lithium battery anodes," *Nature Nanotechnol.*, vol. 9, no. 3, pp. 187–192, 2014.

[60] A. Khaligh and Z. Li, "Battery, ultracapacitor, fuel cell, and hybrid energy storage systems for electric, hybrid electric, fuel cell, and plug-in hybrid electric vehicles: State of the art," *IEEE Trans. Veh. Technol.*, vol. 59, no. 6, pp. 2806–2814, Jul. 2010.

[61] T. B. Reddy, *Linden's Handbook of Batteries*, 4th ed. New York, NY, USA: McGraw-Hill, 2010, ch. 39.

[62] A. J. Bard and L. R. Faulkner, *Electrochemical Methods: Fundamentals and Applications*, 2nd ed. New York, NY, USA: Wiley, 2001.

[63] H.-L. Girard, H. Wang, A. L. d'Entremont, and L. Pilon, "Enhancing faradaic charge storage contribution in hybrid pseudocapacitors," *Electrochim. Acta*, vol. 182, pp. 639–651, Nov. 2015.

[64] A. D. Pasquier, I. Plitz, S. Menocal, and G. Amatucci, "A comparative study of Li-ion battery, supercapacitor and nonaqueous asymmetric hybrid devices for automotive applications," *J. Power Sour.*, vol. 115, no. 1, pp. 171–178, Mar. 2003.

[65] B. J. Kirby, *Micro- and Nanoscale Fluid Mechanics: Transport in Microfluidic Devices*. Cambridge, U.K.: Cambridge Univ. Press, 2010.

[66] A. Burke, M. Miller, and H. Zhao, "Ultracapacitors in hybrid vehicle applications: Testing of new high power devices and prospects for increased energy density," in *Proc. 26th Electr. Vehicle Symp. (EVS)*, vol. 3. 2012, pp. 2213–2220.

[67] A. Lajunen, "Energy consumption and cost-benefit analysis of hybrid and electric city buses," *Transp. Res. C, Emerg. Technol.*, vol. 38, pp. 1–15, Jan. 2014.

[68] A. Affanni, A. Bellini, G. Franceschini, P. Guglielmi, and C. Tassoni, "Battery choice and management for new-generation electric vehicles," *IEEE Trans. Ind. Electron.*, vol. 52, no. 5, pp. 1343–1349, Oct. 2005.

[69] S. M. Lukic, J. Cao, R. C. Bansal, F. Rodriguez, and A. Emadi, "Energy storage systems for automotive applications," *IEEE Trans. Ind. Electron.*, vol. 55, no. 6, pp. 2258–2267, Jun. 2008.

[70] G. Berdichevsky, K. Kelty, J. B. Straubel, and E. Toomre, "The tesla roadster battery system," Tesla Motors, San Carlos, CA, USA, Tech. Rep., 2006.

[71] D. H. Doughty and C. C. Crafts, "FreedomCAR electrical energy storage system abuse test manual for electric and hybrid electric vehicle applications," United States Council Automotive Res., Southfield, MI, USA, Tech. Rep. SAND2005-3123, 2005, pp. 3–48.

[72] *K2 Ultracapacitors—2.7V Series*, document 1015370.5, Maxwell, 2014. [Online]. Available: http://www.maxwell.com/images/documents/K2Series_DS_1015370_5_20141104.pdf

[73] JM Energy Corporation. (2014). *Lithium Ion Capacitor ULTIMO*. [Online]. Available: http://www.jsrmicro.com/docs/ULTIMO%20Brocure-en.pdf

[74] J. Cao, N. Schofield, and A. Emadi, "Battery balancing methods: A comprehensive review," in *Proc. IEEE Vehicle Power Propuls. Conf. (VPPC)*, Sep. 2008, pp. 1–6.

[75] N. H. Kutkut, H. L. N. Wiegman, D. M. Divan, and D. W. Novotny, "Charge equalization for an electric vehicle battery system," *IEEE Trans. Aerosp. Electron. Syst.*, vol. 34, no. 1, pp. 235–246, Jan. 1998.

[76] N. H. Kutkut, H. L. N. Wiegman, D. M. Divan, and D. W. Novotny, "Design considerations for charge equalization of an electric vehicle battery system," *IEEE Trans. Ind. Electron.*, vol. 35, no. 1, pp. 28–35, Jan./Feb. 1999.

[77] W. Peukert, "Über die Abhängigkeit der Kapazität von der Entladestromstärke bei Bleiakkumulatoren," *Elektrotechnische Zeitschrift*, vol. 20, pp. 20–21, 1897.

[78] D. Doerffel and S. A. Sharkh, "A critical review of using the Peukert equation for determining the remaining capacity of lead-acid and lithium-ion batteries," *J. Power Sour.*, vol. 155, no. 2, pp. 395–400, 2006.

[79] A. Hausmann and C. Depcik, "Expanding the Peukert equation for battery capacity modeling through inclusion of a temperature dependency," *J. Power Sour.*, vol. 235, pp. 148–158, Aug. 2013.

[80] S. Peck and M. Pierce, "Development of a temperature-dependent Li-ion battery thermal model," SAE Tech. Paper 2012-01-0117, 2012.

[81] L. Gao, S. Liu, and R. A. Dougal, "Dynamic lithium-ion battery model for system simulation," *IEEE Trans. Compon. Packag. Technol.*, vol. 25, no. 3, pp. 495–505, Sep. 2002.

[82] C. K. Dyer, P. T. Moseley, Z. Ogumi, D. A. J. Rand, and B. Scrosati, *Encyclopedia of Electrochemical Power Sources*. Amsterdam, The Netherlands: Elsevier, 2009.

[83] J. Vetter *et al.*, "Ageing mechanisms in lithium-ion batteries," *J. Power Sour.*, vol. 147, nos. 1–2, pp. 269–281, 2005.

[84] M. Broussely *et al.*, "Main aging mechanisms in Li ion batteries," *J. Power Sour.*, vol. 146, nos. 1–2, pp. 90–96, 2005.

[85] A. Farmann, W. Waag, A. Marongiu, and D. U. Sauer, "Critical review of on-board capacity estimation techniques for lithium-ion batteries in electric and hybrid electric vehicles," *J. Power Sour.*, vol. 281, pp. 114–130, May 2015.

[86] S. M. Rezvanizaniani, Z. Liu, Y. Chen, and J. Lee, "Review and recent advances in battery health monitoring and prognostics technologies for electric vehicle (EV) safety and mobility," *J. Power Sour.*, vol. 256, pp. 110–124, Jun. 2014.

[87] A. Barré, B. Deguilhem, S. Grolleau, M. Gérard, F. Suard, and D. Riu, "A review on lithium-ion battery ageing mechanisms and estimations for automotive applications," *J. Power Sour.*, vol. 241, pp. 680–689, Nov. 2013.

[88] W. Waag, C. Fleischer, and D. U. Sauer, "Critical review of the methods for monitoring of lithium-ion batteries in electric and hybrid vehicles," *J. Power Sour.*, vol. 258, pp. 321–339, Jul. 2014.

[89] P. Malysz, R. Gu, J. Ye, H. Yang, and A. Emadi, "State-of-charge and state-of-health estimation with state constraints and current sensor bias correction for electrified powertrain vehicle batteries," *IET Elect. Syst. Transp.*, pp. 1–9, 2016.

[90] I. Snihir, W. Rey, E. Verbitskiy, A. Belfadhel-Ayeb, and P. H. L. Notten, "Battery open-circuit voltage estimation by a method of statistical analysis," *J. Power Sour.*, vol. 159, no. 2, pp. 1484–1487, Sep. 2006.

[91] R. Ahmed, M. El Sayed, I. Arasaratnam, J. Tjong, and S. Habibi, "Reduced-order electrochemical model parameters identification and SOC estimation for healthy and aged Li-ion batteries—Part I: Parameterization model development for healthy batteries," *IEEE J. Emerg. Sel. Topics Power Electron.*, vol. 2, no. 3, pp. 659–677, Sep. 2014.

[92] R. Ahmed, M. El Sayed, I. Arasaratnam, J. Tjong, and S. Habibi, "Reduced-order electrochemical model parameters identification and state of charge estimation for healthy and aged Li-ion batteries—Part II: Aged battery model and state of charge estimation," *IEEE J. Emerg. Sel. Topics Power Electron.*, vol. 2, no. 3, pp. 678–690, Sep. 2014.

[93] F. Codecà, S. M. Savaresi, and V. Manzoni, "The mix estimation algorithm for battery state-of-charge estimator—Analysis of the sensitivity to measurement errors," in *Proc. 48th IEEE Conf. Decision Control, 28th Chin. Control Conf. (CDC/CCC)*, Dec. 2009, pp. 8083–8088.

[94] F. Codecà, S. M. Savaresi, and G. Rizzoni, "On battery state of charge estimation: A new mixed algorithm," in *Proc. 17th IEEE Int. Conf. Control Appl. (CCA)*, Sep. 2008, pp. 102–107.

[95] M. A. Roscher, "Zustandserkennung von $LiFePO_4$-batterien für hybrid- und elektrofahrzeuge," Ph.D. dissertation, RWTH Aachen Univ., Aachen, Germany, 2010.

[96] M. A. Roscher and D. U. Sauer, "Dynamic electric behavior and open-circuit-voltage modeling of $LiFePO_4$-based lithium ion secondary batteries," *J. Power Sour.*, vol. 196, no. 1, pp. 331–336, 2011.

[97] F. Baronti *et al.*, "State-of-charge estimation enhancing of lithium batteries through a temperature-dependent cell model," in *Proc. Int. Conf. Appl. Electron. (AE)*, Sep. 2011, pp. 1–5.

[98] M. A. Roscher, O. S. Bohlen, and D. U. Sauer, "Reliable state estimation of multicell lithium-ion battery systems," *IEEE Trans. Energy Convers.*, vol. 26, no. 3, pp. 737–743, Sep. 2011.

[99] T. Kim, W. Qiao, and L. Qu, "Real-time state of charge and electrical impedance estimation for lithium-ion batteries based on a hybrid battery model," in *Proc. 28th Annu. IEEE Appl. Power Electron. Conf. Expo. (APEC)*, Mar. 2013, pp. 563–568.

[100] T. Kim, W. Qiao, and L. Qu, "Online state of charge and electrical impedance estimation for multicell lithium-ion batteries," in *Proc. IEEE Transp. Electrific. Conf. Expo (ITEC)*, Jun. 2013, pp. 1–6.

[101] J. Li, J. K. Barillas, C. Guenther, and M. A. Danzer, "A comparative study of state of charge estimation algorithms for $LiFePO_4$ batteries used in electric vehicles," *J. Power Sour.*, vol. 230, pp. 244–250, May 2013.

[102] X. Hu, F. Sun, and Y. Zou, "Estimation of state of charge of a lithium-ion battery pack for electric vehicles using an adaptive Luenberger observer," *Energies*, vol. 3, no. 9, pp. 1586–1603, 2010.

[103] H. Chaoui and P. Sicard, "Accurate state of charge (SOC) estimation for batteries using a reduced-order observer," in *Proc. IEEE Int. Conf. Ind. Technol. (ICIT)*, Mar. 2011, pp. 39–43.

[104] L. Liu, L. Y. Wang, Z. Chen, C. Wang, F. Lin, and H. Wang, "Integrated system identification and state-of-charge estimation of battery systems," *IEEE Trans. Energy Convers.*, vol. 28, no. 1, pp. 12–23, Mar. 2013.

[105] Y.-H. Chiang, W.-Y. Sean, and J.-C. Ke, "Online estimation of internal resistance and open-circuit voltage of lithium-ion batteries in electric vehicles," *J. Power Sour.*, vol. 196, no. 8, pp. 3921–3932, 2011.

[106] M. Gholizadeh and F. R. Salmasi, "Estimation of state of charge, unknown nonlinearities, and state of health of a lithium-ion battery based on a comprehensive unobservable model," *IEEE Trans. Ind. Electron.*, vol. 61, no. 3, pp. 1335–1344, Mar. 2014.

[107] I.-S. Kim, "The novel state of charge estimation method for lithium battery using sliding mode observer," *J. Power Sour.*, vol. 163, no. 1, pp. 584–590, 2006.

[108] F. Zhang, G. Liu, and L. Fang, "A battery state of charge estimation method using sliding mode observer," in *Proc. 7th World Congr. Intell. Control Autom.*, 2008, pp. 989–994.

[109] X. Chen, W. Shen, Z. Cao, A. Kapoor, and I. Hijazin, "Adaptive gain sliding mode observer for state of charge estimation based on combined battery equivalent circuit model in electric vehicles," in *Proc. 8th IEEE Conf. Ind. Electron. Appl. (ICIEA)*, Jun. 2013, pp. 601–606.

[110] X. Chen, W. Shen, Z. Cao, and A. Kapoor, "A novel approach for state of charge estimation based on adaptive switching gain sliding mode observer in electric vehicles," *J. Power Sour.*, vol. 246, pp. 667–678, Jan. 2014.

[111] G. L. Plett, "Extended Kalman filtering for battery management systems of LiPB-based HEV battery packs: Part 1. Background," *J. Power Sour.*, vol. 134, pp. 252–261, Aug. 2004.

[112] G. L. Plett, "Extended Kalman filtering for battery management systems of LiPB-based HEV battery packs: Part 2. Modeling and identification," *J. Power Sour.*, vol. 134, no. 2, pp. 262–276, 2004.

[113] G. L. Plett, "Extended Kalman filtering for battery management systems of LiPB-based HEV battery packs: Part 3. State and parameter estimation," *J. Power Sour.*, vol. 134, no. 2, pp. 277–292, 2004.

[114] S. E. Samadani, R. A. Fraser, and M. Fowler, "A review study of methods for lithium-ion battery health monitoring and remaining life estimation in hybrid electric vehicles," SAE Tech. Paper 2012-01-0125, 2012.

[115] M. Chen and G. A. Rincón-Mora, "Accurate electrical battery model capable of predicting runtime and I–V performance," *IEEE Trans. Energy Convers.*, vol. 21, no. 2, pp. 504–511, Jun. 2006.

[116] E. Chemali *et al.*, "Minimizing battery wear in a hybrid energy storage system using a linear quadratic regulator," in *Proc. 41st Annu. Conf. IEEE Ind. Electron. Soc. (IECON)*, Nov. 2015, pp. 003265–003270.

[117] S. Buller, M. Thele, R. W. De Doncker, and E. Karden, "Impedance-based simulation models of supercapacitors and Li-ion batteries for power electronic applications," in *Proc. 38th IAS Annu. Meeting. Conf. Rec. Ind. Appl. Conf.*, vol. 3. Oct. 2003, pp. 1596–1600.

[118] D. Andre, M. Meiler, K. Steiner, H. Walz, T. Soczka-Guth, and D. U. Sauer, "Characterization of high-power lithium-ion batteries by electrochemical impedance spectroscopy. II: Modelling," *J. Power Sour.*, vol. 196, no. 12, pp. 5349–5356, 2011.

[119] W. Wang, J. Ye, P. Malysz, H. Yang, and A. Emadi, "Sensitivity analysis of Kalman filter based capacity estimation for electric vehicles," in *Proc. IEEE Transp. Electrific. Conf. Expo (ITEC)*, Jun. 2015, pp. 1–7.

[120] P. Malysz, J. Ye, R. Gu, H. Yang, and A. Emadi, "Battery state-of-power peak current calculation and verification using an asymmetric parameter equivalent circuit model," *IEEE Trans. Veh. Technol.*, vol. 65, no. 6, pp. 4512–4522, Jun. 2016.

[121] H. J. Bergveld, "Battery management systems design by modelling," Ph.D. dissertation, Univ. Twente, Enschede, The Netherlands, 2001.

[122] V. Pop, H. J. Bergveld, D. Danilov, P. P. L. Regtien, and P. H. L. Notten, *Battery Management Systems: Accurate State-of-Charge Indication for Battery-Powered Applications*. London, U.K.: Springer-Verlag, 2008.

[123] J. T. B. A. Kessels, B. Rosca, H. J. Bergveld, and P. P. J. van den Bosch, "On-line battery identification for electric driving range prediction," in *Proc. IEEE Vehicle Power Propuls. Conf. (VPPC)*, Sep. 2011, pp. 1–6.

[124] E. Barsoukov, D. Poole, and D. Freeman, "Circuit and method for measurement of battery capacity fade," U.S. Patent 6 892 148, May 10, 2005.

[125] X. Zhang, X. Tang, J. Lin, Y. Zhang, M. A. Salman, and Y.-K. Chin, "Method for battery capacity estimation," U.S. Patent 8 084 996, Dec. 27, 2011.

[126] B. S. Bhangu, P. Bentley, D. A. Stone, and C. M. Bingham, "Nonlinear observers for predicting state-of-charge and state-of-health of lead-acid batteries for hybrid-electric vehicles," *IEEE Trans. Veh. Technol.*, vol. 54, no. 3, pp. 783–794, May 2005.

[127] B. S. Bhangu, P. Bentley, D. A. Stone, and C. M. Bingham, "State-of-charge and state-of-health prediction of lead-acid batteries for hybrid electric vehicles using non-linear observers," in *Proc. IEEE 11th Eur. Conf. Power Electron. Appl.*, Sep. 2005, p. 10.

[128] F. Zhang, G. Liu, and L. Fang, "Battery state estimation using unscented Kalman filter," in *Proc. IEEE Int. Conf. Robot. Autom. (ICRA)*, May 2009, pp. 1863–1868.

[129] X. Tang, X. Mao, J. Lin, and B. Koch, "Capacity estimation for Li-ion batteries," in *Proc. Amer. Control Conf.*, 2011, pp. 947–952.

[130] X. Tang, Y. Zhang, A. C. Baughman, B. J. Koch, J. Lin, and D. R. Frisch, "Dynamic battery capacity estimation," U.S. Patent 0 136 594, May 31, 2012.

[131] G. L. Plett, "Sigma-point Kalman filtering for battery management systems of LiPB-based HEV battery packs: Part 2: Simultaneous state and parameter estimation," *J. Power Sour.*, vol. 161, no. 2, pp. 1369–1384, 2006.

[132] V. J. Bigorra, R. J. Giro, V. M. Puig, S. O. Ruiz, and M. J. Samitier, "System for dynamic evaluation of the state of health and charge of a vehicle battery," EP Patent 1 357 390, Oct. 29, 2003.

[133] K. S. Champlin, "Method and apparatus for determining battery properties from complex impedance/admittance," U.S. Patent 6 037 777, Mar. 14, 2000.

[134] J. S. Marti, M. P. Vidal, O. R. Sanchez, D. G. Murillo, J. B. Vives, and J. G. Roca, "Method for dynamically measuring the state of health and charge of a car battery and device for implementing said method," U.S. Patent 6 876 174, Apr. 5, 2005.

[135] S. Pang, J. Farrell, J. Du, and M. Barth, "Battery state-of-charge estimation," in *Proc. Amer. Control Conf. (ACC)*, vol. 2. Jun. 2001, pp. 1644–1649.

[136] H. Dai, X. Wei, and Z. Sun, "State and parameter estimation of a HEV Li-ion battery pack using adaptive Kalman filter with a new SOC-OCV concept," in *Proc. Int. Conf. Meas. Technol. Mechatronics Autom.*, vol. 2. Apr. 2009, pp. 375–380.

[137] H. He, R. Xiong, and H. Guo, "Online estimation of model parameters and state-of-charge of $LiFePO_4$ batteries in electric vehicles," *Appl. Energy*, vol. 89, no. 1, pp. 413–420, Jan. 2012.

[138] D. V. Do, C. Forgez, K. E. K. Benkara, and G. Friedrich, "Impedance observer for a Li-ion battery using Kalman filter," *IEEE Trans. Veh. Technol.*, vol. 58, no. 8, pp. 3930–3937, Oct. 2009.

[139] G. Plett, "State and parameter estimation for an electrochemical cell," U.S. Patent 8 103 485, Jan. 24, 2012.

[140] X.-S. Hu, F.-C. Sun, and X. Cheng, "Recursive calibration for a lithium iron phosphate battery for electric vehicles using extended Kalman filtering," *J. Zhejiang Univ. Sci. A*, vol. 12, no. 11, pp. 818–825, 2011.

[141] D. Haifeng, W. Xuezhe, and S. Zechang, "A new SOH prediction concept for the power lithium-ion battery used on HEVs," in *Proc. IEEE Vehicle Power Propuls. Conf. (VPPC)*, Sep. 2009, pp. 1649–1653.

[142] R. Xiong, F. Sun, X. Gong, and C. Gao, "A data-driven based adaptive state of charge estimator of lithium-ion polymer battery used in electric vehicles," *Appl. Energy*, vol. 113, pp. 1421–1433, Jan. 2014.

[143] H. He, X. Zhang, R. Xiong, Y. Xu, and H. Guo, "Online model-based estimation of state-of-charge and open-circuit voltage of lithium-ion batteries in electric vehicles," *Energy*, vol. 39, no. 1, pp. 310–318, Mar. 2012.

[144] J. Li, J. K. Barillas, C. Guenther, and M. A. Danzer, "Sequential Monte Carlo filter for state estimation of $LiFePO_4$ batteries based on an online updated model," *J. Power Sour.*, vol. 247, pp. 156–162, Feb. 2014.

[145] P. Cicconi, D. Landi, A. Morbidoni, and M. Germani, "Feasibility analysis of second life applications for Li-ion cells used in electric powertrain using environmental indicators," in *Proc. IEEE Int. Energy Conf. Exhibit. (ENERGYCON)*, Sep. 2012, pp. 985–990.

[146] N. H. Kutkut and D. M. Divan, "Dynamic equalization techniques for series battery stacks," in *Proc. Int. Telecommun. Energy Conf. (INTELEC)*, Oct. 1996, pp. 514–521.

[147] C. S. Moo, Y.-C. Hsieh, I. S. Tsai, and J. C. Cheng, "Dynamic charge equalisation for series-connected batteries," *IEE Proc.-Electr. Power Appl.*, vol. 150, no. 5, pp. 501–505, Sep. 2003.

[148] M. Tang and T. Stuart, "Selective buck-boost equalizer for series battery packs," *IEEE Trans. Aerosp. Electron. Syst.*, vol. 36, no. 1, pp. 201–211, Jan. 2000.

[149] S. Moore and P. Schneider, "A review of cell equalization methods for lithium ion and lithium polymer battery systems," SAE Tech. Paper 2001-01-0959, 2001.

[150] W. C. Lee, D. Drury, and P. Mellor, "Comparison of passive cell balancing and active cell balancing for automotive batteries," in *Proc. Vehicle Power Propuls. Conf. (VPPC)*, Sep. 2011, pp. 1–7.

[151] M. Preindl, C. Danielson, and F. Borrelli, "Performance evaluation of battery balancing hardware," in *Proc. Eur. Control Conf. (ECC)*, Jul. 2013, pp. 4065–4070.

[152] L. C. Rosario, "Power and energy management of multiple energy storage systems in electric vehicles," Ph.D. dissertation, Dept. Aerosp. Power Sensors, Cranfield Univ., Cranfield, U.K., 2008.

[153] E. Karden, S. Ploumen, B. Fricke, T. Miller, and K. Snyder, "Energy storage devices for future hybrid electric vehicles," *J. Power Sour.*, vol. 168, no. 1, pp. 2–11, May 2007.

[154] N. Schofield, H. T. Yap, and C. M. Bingham, "Hybrid energy sources for electric and fuel cell vehicle propulsion," in *Proc. IEEE Conf. Vehicle Power Propuls.*, Sep. 2005, pp. 522–529.

[155] A. S. Samosir and A. H. M. Yatim, "Implementation of dynamic evolution control of bidirectional DC–DC converter for interfacing ultracapacitor energy storage to fuel-cell system," *IEEE Trans. Ind. Electron.*, vol. 57, no. 10, pp. 3468–3473, Oct. 2010.

[156] A. Dhand and K. Pullen, "Characterization of flywheel energy storage system for hybrid vehicles," SAE Tech. Paper 2014-01-1796, 2014.

[157] A. Dhand and K. Pullen, "Review of battery electric vehicle propulsion systems incorporating flywheel energy storage," *Int. J. Automotive Technol.*, vol. 16, no. 3, pp. 487–500, Jun. 2015.

[158] R. Gu, P. Malysz, and A. Emadi, "A novel battery/ ultracapacitor hybrid energy storage system analysis based on physics-based lithium-ion battery modeling," in *Proc. IEEE Transp. Electrific. Conf. Expo (ITEC)*, Jun. 2015, pp. 1–6.

[159] F. Blaabjerg, Z. Chen, and S. B. Kjaer, "Power electronics as efficient interface in dispersed power generation systems," *IEEE Trans. Power Electron.*, vol. 19, no. 5, pp. 1184–1194, Sep. 2004.

[160] M. E. Glavin, P. K. W. Chan, S. Armstrong, and W. G. Hurley, "A stand-alone photovoltaic supercapacitor battery hybrid energy storage system," in *Proc. 13th Power Electron. Motion Control Conf. (EPE-PEMC)*, Sep. 2008, pp. 1688–1695.

[161] W. Li and G. Joos, "A power electronic interface for a battery supercapacitor hybrid energy storage system for wind applications," in *Proc. IEEE Power Electron. Specialists Conf. (PESC)*, Jun. 2008, pp. 1762–1768.

[162] A. Etxeberria, I. Vechiu, H. Camblong, and J.-M. Vinassa, "Comparison of three topologies and controls of a hybrid energy storage system for microgrids," *Energy Convers. Manage.*, vol. 54, no. 1, pp. 113–121, Feb. 2012.

[163] H. A. Borhan and A. Vahidi, "Model predictive control of a power-split hybrid electric vehicle with combined battery and ultracapacitor energy storage," in *Proc. Amer. Control Conf. (ACC)*, Jun./Jul. 2010, pp. 5031–5036.

[164] J. Cao, B. Cao, Z. Bai, and W. Chen, "Energy-regenerative fuzzy sliding mode controller design for ultracapacitor-battery hybrid power of electric vehicle," in *Proc. IEEE Int. Conf. Mechatronics Autom.*, Aug. 2007, pp. 1570–1575.

[165] K. Kawashima, T. Uchida, and Y. Hori, "Development of a novel ultracapacitor electric vehicle and methods to cope with voltage variation," in *Proc. 5th IEEE Vehicle Power Propuls. Conf. (VPPC)*, Sep. 2009, pp. 724–729.

[166] V. A. Shah, S. G. Karndhar, R. Maheshwari, P. Kundu, and H. Desai, "An energy management system for a battery ultracapacitor hybrid electric vehicle," in *Proc. Int. Conf. Ind. Inf. Syst. (ICIIS)*, Dec. 2009, pp. 408–413.

[167] A. M. Jarushi and N. Schofield, "Battery and supercapacitor combination for a series hybrid electric vehicle," in *Proc. 5th IET Int. Conf. Power Electron., Mach. Drives (PEMD)*, Apr. 2010, pp. 1–6.
[168] C. Capasso, V. Sepe, O. Veneri, M. Montanari, and L. Poletti, "Experimentation with a ZEBRA plus EDLC based hybrid storage system for urban means of transport," in *Proc. Int. Conf. Elect. Syst. Aircraft, Railway Ship Propuls. (ESARS)*, Mar. 2015, pp. 1–6.
[169] A. Brett, P. Aguiar, and N. P. Brandon, "System modelling and integration of an intermediate temperature solid oxide fuel cell and ZEBRA battery for automotive applications," *J. Power Sour.*, vol. 163, no. 1, pp. 514–522, Dec. 2006.
[170] M. Safari, M. Morcrette, A. Teyssot, and C. Delacourt, "Multimodal physics-based aging model for life prediction of Li-ion batteries," *J. Electrochem. Soc.*, vol. 156, no. 3, pp. A145–A153, 2009.
[171] P. Ramadass, B. Haran, P. M. Gomadam, R. White, and B. N. Popov, "Development of first principles capacity fade model for Li-ion cells," *J. Electrochem. Soc.*, vol. 151, no. 2, pp. A196–A203, 2004.
[172] X. Lin, J. Park, L. Liu, Y. Lee, A. M. Sastry, and W. Lu, "A comprehensive capacity fade model and analysis for Li-ion batteries," *J. Electrochem. Soc.*, vol. 160, no. 10, pp. A1701–A1710, 2013.
[173] M. Safari, M. Morcrette, A. Teyssot, and C. Delacourt, "Life prediction methods for lithium-ion batteries derived from a fatigue approach," *J. Electrochem. Soc.*, vol. 157, no. 7, pp. A892–A898, 2010.
[174] X. Hu, L. Johannesson, N. Murgovski, and B. Egardt, "Longevity-conscious dimensioning and power management of the hybrid energy storage system in a fuel cell hybrid electric bus," *Appl. Energy*, vol. 137, pp. 913–924, Jan. 2015.
[175] Y. Wang, X. Lin, Q. Xie, N. Chang, and M. Pedram, "Minimizing state-of-health degradation in hybrid electrical energy storage systems with arbitrary source and load profiles," in *Proc. Design, Autom. Test Eur. Conf. Exhibit. (DATE)*, Mar. 2014, pp. 1–4.
[176] A. Santucci, A. Sorniotti, and C. Lekakou, "Power split strategies for hybrid energy storage systems for vehicular applications," *J. Power Sour.*, vol. 258, pp. 395–407, Jul. 2014.
[177] M. B. Camara, H. Gualous, F. Gustin, and A. Berthon, "Design and new control of DC/DC converters to share energy between supercapacitors and batteries in hybrid vehicles," *IEEE Trans. Veh. Technol.*, vol. 57, no. 5, pp. 2721–2735, Sep. 2008.
[178] Z. Song, H. Hofmann, J. Li, J. Hou, X. Han, and M. Ouyang, "Energy management strategies comparison for electric vehicles with hybrid energy storage system," *Appl. Energy*, vol. 134, pp. 321–331, Dec. 2014.
[179] A. Ostadi, M. Kazerani, and S.-K. Chen, "Hybrid energy storage system (HESS) in vehicular applications: A review on interfacing battery and ultra-capacitor units," in *Proc. IEEE Transp. Electrific. Conf. Expo (ITEC)*, Jun. 2013, pp. 1–7.
[180] L. Gao, R. A. Dougal, and S. Liu, "Power enhancement of an actively controlled battery/ultracapacitor hybrid," *IEEE Trans. Power Electron.*, vol. 20, no. 1, pp. 236–243, Jan. 2005.
[181] G. Nielson and A. Emadi, "Hybrid energy storage systems for high-performance hybrid electric vehicles," in *Proc. IEEE Vehicle Power Propuls. Conf.*, Sep. 2011, pp. 1–6.
[182] A. Kuperman, I. Aharon, S. Malki, and A. Kara, "Design of a semiactive battery-ultracapacitor hybrid energy source," *IEEE Trans. Power Electron.*, vol. 28, no. 2, pp. 806–815, Feb. 2013.
[183] J. Cao and A. Emadi, "A new battery/ultra-capacitor hybrid energy storage system for electric, hybrid and plug-in hybrid electric vehicles," in *Proc. IEEE Vehicle Power Propuls. Conf.*, Sep. 2009, pp. 941–946.
[184] K. Zhuge and M. Kazerani, "Development of a hybrid energy storage system (HESS) for electric and hybrid electric vehicles," in *Proc. IEEE Transp. Electrific. Conf. Expo (ITEC)*, Jun. 2014, pp. 1–5.
[185] J. Cao and A. Emadi, "A new battery/ultracapacitor hybrid energy storage system for electric, hybrid, and plug-in hybrid electric vehicles," *IEEE Trans. Power Electron.*, vol. 27, no. 1, pp. 122–132, Jan. 2012.
[186] J. M. Miller, U. Deshpande, T. J. Dougherty, and T. Bohn, "Power electronic enabled active hybrid energy storage system and its economic viability," in *Proc. IEEE Appl. Power Electron. Conf. Expo. (APEC)*, Feb. 2009, pp. 190–198.
[187] J. M. Blanes, R. Gutiérrez, A. Garrigós, J. L. Lizán, and J. M. Cuadrado, "Electric vehicle battery life extension using ultracapacitors and an FPGA controlled interleaved buck–boost converter," *IEEE Trans. Power Electron.*, vol. 28, no. 12, pp. 5940–5948, Dec. 2013.
[188] C.-H. Tu and A. Emadi, "A novel series-parallel reconfigurable hybrid energy storage system for electrified vehicles," in *Proc. IEEE Transp. Electrific. Conf. Expo (ITEC)*, Jun. 2012, pp. 1–4.

Ephrem Chemali (S'14) received the B.Sc. (Hons.) degree in physics and the M.Sc. degree in atomic physics from York University, Toronto, ON, Canada, in 2009 and 2011, respectively. He is currently pursuing the Ph.D. degree with the McMaster Institute for Automotive Research and Technology (MacAUTO), McMaster University, Hamilton, ON, Canada.

He was an Engineering Lead and a Project Manager of Moose Power, Toronto, a photovoltaic solar rooftop developer, where he managed the interconnection of 1.7 MW of rooftop solar projects, after completing his M.Sc. studies. Since 2014, he has served as the Energy Storage System Team Lead for the McMaster Engineering EcoCAR 3 team. He is involved in research on modeling, designing, and building next generation energy storage systems, dc/dc converters, and inverters for electric drive vehicles with MacAUTO. His current research interests include next generation energy storage systems and power electronics for electrified transportation applications and smart grid technologies.

Mr. Chemali's M.Sc. project on precision spectroscopy of lithium ions received the DAMPhi Award at the Canadian Association of Physicists Conference in 2010. In 2010, he was a recipient of the Ralph Nicolls Award for Science Communication at York University.

Matthias Preindl (S'12–M'15) received the B.Sc. (*summa cum laude*) degree in electrical engineering from the University of Padua, Padua, Italy, in 2008, the M.Sc. degree in electrical engineering and information technology from ETH Zurich, Zurich, Switzerland, in 2010, and the Ph.D. degree in energy engineering from the Doctoral School of Industrial Engineering, University of Padua, in 2014.

He was a Trainee with the National Research Council, Rome, Italy, in 2008, a Visiting Student with Aalborg University, Aalborg, Denmark, in 2009, and a Visiting Scholar with the University of California at Berkeley, Berkeley, CA, USA, in 2013. He was with Leitwind AG, Sterzing, Italy, as a Research and Development Engineer in Power Electronic and Drives from 2010 to 2012. He was a Post-Doctoral Research Associate with the McMaster Institute for Automotive Research and Technology, McMaster University, Hamilton, ON, Canada, from 2014 to 2015, where he was a Sessional Professor with the Department of Electrical and Computer Engineering in 2015. He is currently an Assistant Professor with the Department of Electrical Engineering, Columbia University, New York, NY, USA. He actively collaborates with industry partners on a project basis. His current research interests include the design and control of power electronic and motor drive systems with applications in electrified transportation systems, renewable-energy power plants, and smart grids.

Dr. Preindl received several honors, including merit-based fellow and scholarships, a price for outstanding achievements during his studies, and best presentation awards.

Pawel Malysz (S'06–M'12) received the B.Eng. degree in engineering physics and the M.A.Sc. and Ph.D. degrees in electrical engineering from McMaster University, Hamilton, ON, Canada, in 2005, 2007, and 2011, respectively.

He was a Biomedical Engineering Intern with the Juravinski Cancer Centre, Hamilton, from 2003 to 2004. From 2012 to 2014, he was a Principal Research Engineer with the McMaster Institute for Automotive Research and Technology, McMaster University, a Canada Excellence Research Centre. In 2015, he was appointed as an Adjunct Assistant Professor with the Department of Electrical and Computer Engineering, McMaster University. He is currently a Battery Management Systems Control Engineer with Fiat Chrysler Automobiles, Auburn Hills, MI, USA. His current research interests include energy systems, battery management software design, electrified transportation, haptics, robotics, and advanced control engineering.

Dr. Malysz co-received the Chrysler Innovation Award in 2014. He is an Associate Editor of *IET Power Electronics* and a Licensed Professional Engineer in the province of Ontario.

Ali Emadi (S'98–M'00–SM'03–F'13) received the B.S. and M.S. (Hons.) degrees from the Sharif University of Technology, Tehran, Iran, in 1995 and 1997, respectively, and the Ph.D. degree from Texas A&M University, College Station, TX, USA, in 2000, all in electrical engineering.

He was the Harris Perlstein Endowed Chair Professor of Engineering and the Director of the Electric Power and Power Electronics Center and Grainger Laboratories with the Illinois Institute of Technology (IIT), Chicago, IL, USA, where he established research and teaching facilities as well as courses in power electronics, motor drives, and vehicular power systems. He was the Founder, Chairman, and President of Hybrid Electric Vehicle Technologies, Inc., Chicago, a university spin-off company of IIT. He is currently the Canada Excellence Research Chair in Hybrid Powertrain with McMaster University, Hamilton, ON, Canada. He has authored or co-authored over 350 journal and conference papers and several books, including *Vehicular Electric Power Systems* (2003), *Energy Efficient Electric Motors* (2004), *Uninterruptible Power Supplies and Active Filters* (2004), *Modern Electric, Hybrid Electric, and Fuel Cell Vehicles—Second Edition* (2009), and *Integrated Power Electronic Converters and Digital Control* (2009). He is also the Editor of the *Handbook of Automotive Power Electronics and Motor Drives* (2005) and *Advanced Electric Drive Vehicles (2014)*.

Dr. Emadi has been a recipient of numerous awards and recognitions. He was the Advisor for the Formula Hybrid Teams at IIT and McMaster University, which received the GM Best Engineered Hybrid System Award at the 2010, 2013, and 2015 competitions. He was the Inaugural General Chair of the 2012 IEEE Transportation Electrification Conference and Expo, and has chaired several IEEE and SAE conferences in the areas of vehicle power and propulsion. He is the Founding Editor-in-Chief of the IEEE TRANSACTIONS ON TRANSPORTATION ELECTRIFICATION.